Structure-Based Design of Novel Inhibitors of the MDM2−p53 Interaction

Yosup Rew,[†] Daqing Sun,*,[†] Felix Gonzalez-Lopez De Turiso,[†] Michael D. Bartberger,[∥] Hilary P. Beck,[†] Jude Canon,[⊥] Ada Chen,[†] David Chow,[†] Jeffrey Deignan,[†] Brian M. Fox,[†] Darin Gustin,[†] Xin Huang,[#] Min Jiang,[§] Xianyun Jiao,[†] Lixia Jin,[§] Frank Kayser,[†] David J. Kopecky,[†] Yihong Li,[†] Mei-Chu Lo,[†] Alexander M. Long,[#] Klaus Michelsen,[∥] Jonathan D. Oliner,[⊥] Tao Osgood,[⊥] Mark Ragains,[‡] Anne Y. Saiki,[⊥] Steve Schneider,[#] Maria Toteva,[‡] Peter Yakowec,[#] Xuelei Yan,[†] Qiuping Ye,[§] Dongyin Yu,[⊥] Xiaoning Zhao,[†] Jing Zhou,[†] Julio C. Medina,[†] and Steven H. Olson[†]

Departments of [†]Therapeutic Discovery, [‡]Pharmaceutics, and [§]Pharmacokinetics and Drug Metabolism, Amgen Inc., 1120 Veterans Boulevard, South San Francisco, California 94080, United States

Departments of [∥]Therapeutic Discovery and [⊥]Oncology Research, Amgen Inc., One Amgen Center Drive, Thousand Oaks, California 91320, United States

[#]Department of Therapeutic Discovery, Amgen Inc., 360 Binney Street Cambridge, Massachusetts 02142, United States

S *Supporting Information*

ABSTRACT: Structure-based rational design led to the discovery of novel inhibitors of the MDM2−p53 protein−protein interaction. The affinity of these compounds for MDM2 was improved through conformational control of both the piperidinone ring and the appended *N*-alkyl substituent. Optimization afforded **29** (AM-8553), a potent and selective MDM2 inhibitor with excellent pharmacokinetic properties and in vivo efficacy.
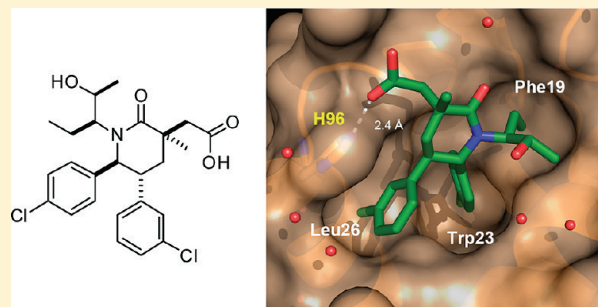
■ INTRODUCTION

The tumor suppressor protein p53 plays a central role in preventing tumor development. Cellular stress in the form of DNA damage, hypoxia, or proapoptotic oncogene activation stimulates p53, resulting in its accumulation in the nucleus. Activated p53 up-regulates the transcription of numerous genes involved in cell cycle arrest, DNA repair, senescence, and apoptosis.[1,2] As a result, inactivation of the p53 pathway in tumor cells provides a strong selective growth advantage, and it has been proposed that elimination of the p53 function may be a requisite step in tumor formation.[3] Recently, three independent studies demonstrated that restoring endogenous p53 function results in tumor regression in vivo and could be an effective anticancer therapeutic approach.[4−7]

The MDM2 (murine double minute 2) oncogene is an important negative regulator of p53. In unstressed cells, a negative feedback loop maintains both p53 and MDM2 at very low levels. MDM2 is transcriptionally activated by p53, and the activity of p53 is regulated by MDM2 through three main mechanisms. First, MDM2 represses p53 transcriptional activity by binding to the p53 transactivation domain. Second, MDM2 transports p53 from the nucleus to the cytosol. Finally, MDM2 functions as an E3 ubiquitin ligase and facilitates the degradation of both p53 and itself in the cellular 26S proteasome.[1,2]

Wild-type p53 is found in approximately 50% of human cancers,[8] and inhibition of the MDM2−p53 interaction with nonpeptidic small-molecule MDM2 inhibitors has been shown to be a tractable mechanism for activation of the p53 pathway.[9] However, targeting a protein−protein interaction with small molecule inhibitors still represents a considerable challenge for drug discovery. The potential binding regions typically involve vast surface areas that contain poorly defined binding regions.[10] As a result, small molecule inhibitors of protein−protein interactions tend to have high molecular weight, and when bound to their target, a considerable fraction of their total surface area is solvent-exposed. These factors can make lead optimization quite formidable. Although researchers have recognized the potential benefits of neutralizing the MDM2−p53 protein−protein interaction for nearly 20 years, to date, only a few molecules have advanced into clinical trials.[11]

Previously, we identified a class of chromenotriazolopyrimidine inhibitors of the MDM2−p53 interaction from high-throughput screening of our chemical library.[12,13] To comple-

ment these efforts, we embarked on a parallel strategy to design, de novo, a new scaffold of MDM2 inhibitors based on the binding mode of known inhibitors with MDM2 (Figure 1).[12,14,15]
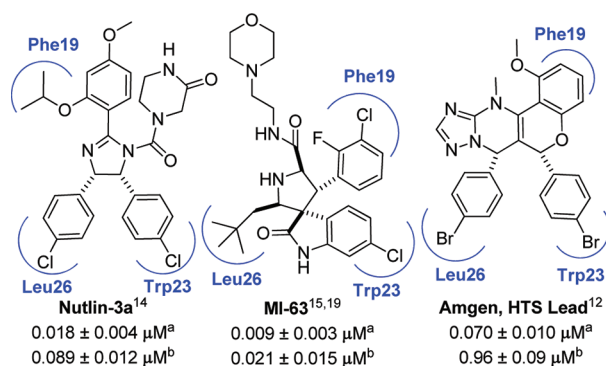

Figure 1. Binding mode of three known MDM2 inhibitors. Blue labels indicate the positions normally occupied by key p53 residues. [a]IC$_{50}$ in biochemical assay (HTRF, serum free). [b]IC$_{50}$ in biochemical assay (HTRF, 15% human serum).

Herein, we describe the discovery of novel scaffolds, exemplified by compounds **1** and **2** in Figure 2, as promising
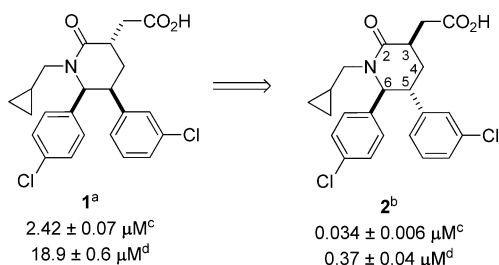

Figure 2. Discovery of novel piperidinone lead **2** from de novo design and synthesis. [a]Racemic mixture. [b]Single enantiomer. [c]IC$_{50}$ in biochemical assay (HTRF, serum free). [d]IC$_{50}$ in biochemical assay (HTRF, 15% human serum).

leads for the inhibition of the MDM2−p53 interaction. Compound **2** exhibits meaningful potency levels in both biochemical (HTRF-based neutralization assay measuring inhibition of the interaction between MDM2 and p53) and cell-based (p21 induction and cell proliferation assays in SJSA-1 tumor cells) assays (Table 2).[16]

Systematic optimization of this novel piperidinone series led to compound **25**, a potent and selective MDM2 inhibitor. Consistent with its mechanism of action, the ability of **25** to inhibit cell proliferation and increase p21 induction of HCT116 p53^{wt} vs HCT116 p53$^{-/-}$ tumor cells confirmed that the activity of this compound is p53 dependent. In addition, compound **25** exhibited both dose-dependent p21 induction and tumor growth inhibition in SJSA-1 tumor xenograft studies. Further optimization of **25** resulted in the discovery of **29** (AM-8553), a molecule with improved potency and pharmacokinetic properties. **29** showed substantially lower intrinsic clearance in human hepatocytes and excellent projected human pharmacokinetic parameters. In alignment with its improved in vitro potency, **29** demonstrated superior efficacy in 14-day SJSA-1 tumor xenograft studies.

RESULTS AND DISCUSSION

The crystal structure of the 109-residue amino-terminal domain of MDM2 bound to a 15-residue transactivation domain peptide of p53 revealed that MDM2 has three hydrophobic clefts that bind three critical residues of p53 (Phe19, Trp23, and Leu26).[17] Because of the central role p53 plays in human cancer and the presence of a relatively well-defined MDM2 binding region, inhibition of the MDM2/p53 protein−protein interaction with low molecular-weight small molecules has been considered a compelling therapeutic target in oncology for the past decade.[9,14,15,18]

On the basis of a structural analysis of known MDM2 inhibitors (Figure 1), several novel scaffolds were conceived.[20] Initial SAR around those scaffolds led to the identification of 1,3,5,6-tetrasubstituted piperidinone **1** (Figure 2), whose IC$_{50}$ in the HTRF assay was 2.42 μM in serum free buffer. Changing the *cis*-diaryl configuration into *trans*-diaryl, inverting the stereochemical configuration of the C3 acetic acid substituent, and resolving/identifying the active enantiomer resulted in a 50- to 70-fold increase in potency (**2** vs **1**).[20]

The predicted binding mode of compound **2**[21] from docking[22] is shown in Figure 3. It was proposed that the
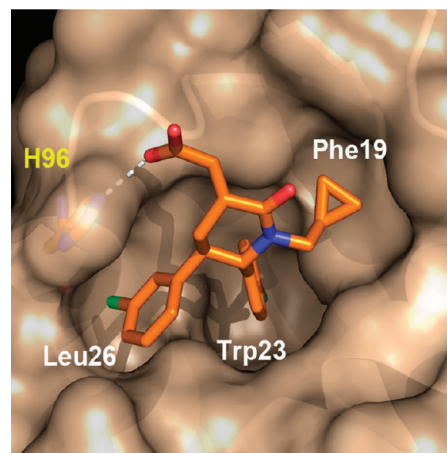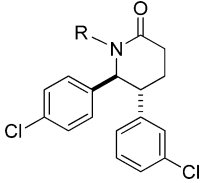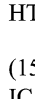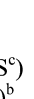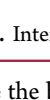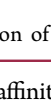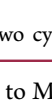

Figure 3. Model of proposed binding mode of compound **2**. MDM2 binding pockets are labeled (by p53 side chain) in white, H96 labeled in yellow.

Leu26$_{(p53)}$ pocket contains the C5 *m*-Cl phenyl substituent, with the deepest Trp23$_{(p53)}$ pocket occupied by the C6 *p*-Cl phenyl group. The cyclopropylmethyl group occupies the Phe19$_{(p53)}$ pocket, while the carboxylate anion forms an electrostatic interaction with the H96 imidazole side chain of MDM2 (Figure 3).

Initial optimization of **2** began with the modification of the N-alkyl group. By use of the minimally substituted piperidinone **3** as a template, several primary alkyl derivatives were rapidly synthesized to optimize the N-alkyl moiety (Table 1, compounds **4**−**8**).

The N-cyclopropylmethyl derivative **4** was the most potent compound among the primary N-alkylpiperidinone derivatives, with a 6-fold improvement over the unsubstituted piperidinone **3**. The n-propyl derivative **5** possessed an activity similar to that of **4**. When the size of the alkyl group was larger than the cyclopropylmethyl or n-propyl, potency decreased (**6**, **7**, and **8**). Resolution of the two enantiomers of **4** demonstrated that only

Table 1. Exploration of the N-Alkyl Group

Compd	R	HTRF IC$_{50}$ (μM)[b]	HTRF (15% HS[c]) IC$_{50}$ (μM)[b]
3[a]	H	10.0 ± 3.6	>30
4[a]	(cyclopropyl)	1.5 ± 0.3	>30
(5R,6S)-4	(cyclopropyl)	0.82 ± 0.28	>30
(5S,6R)-4	enantiomer of (5R,6S)-4	>30	>30
5[a]		1.9 ± 0.5	>30
6[a]		2.3 ± 0.3	>30
7[a]		2.7 ± 0.2	>30
8[a]		5.4 ± 0.9	>30
9[a]		0.94 ± 0.18	18.7 ± 0.8
10[a]		3.5 ± 1.0	>30
11[a]		1.4 ± 0.5	>30
12[a]		1.7 ± 0.4	>30
13[a]		5.5 ± 1.7	>30

[a]Compounds are racemic. [b]Potency data are reported as the average of at least two determinations. [c]HS = human serum.

the (5R,6S)-4 enantiomer exhibited measurable activity [IC$_{50}$ = 0.82 μM; IC$_{50}$ > 30 μM for (5S,6R)-4].

The N-cyclopropylmethyl group of 2 (or 4) likely requires a "downward" orientation into the Phe19$_{(p53)}$ pocket to maximize binding affinity (see Figures 3 and 4). This orientation of the N-alkyl substituent (syn with respect to the nearby p-chlorophenyl) results in destabilization of the desired binding conformer.

It was hypothesized that incorporation of an additional substituent at the methylene adjacent to the ring nitrogen could
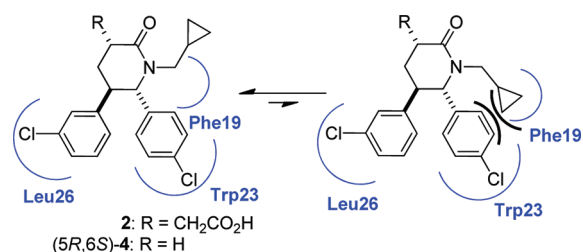
Figure 4. Interconversion of two cyclopropylmethyl conformations.

improve the binding affinity to MDM2 by "directing" the highly flexible N-alkyl group of 2 into the Phe19 pocket. Therefore, a series of α-substituted N-alkyl derivatives were synthesized, and the biochemical activities of these compounds in the HTRF competition assay[16] are summarized in Table 1.

B3LYP/6-31G* analysis of the dihedral profile about the N–C bond of compound 2 demonstrates that the cyclopropylmethyl possesses two local minima (Figure 5a). The
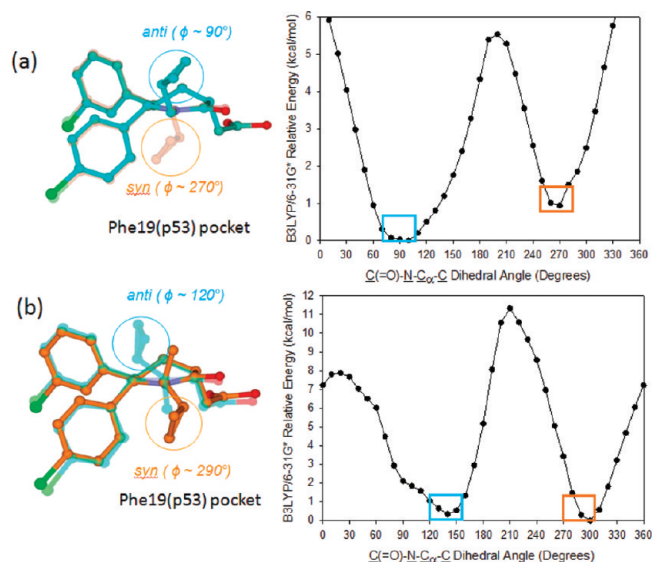
Figure 5. B3LYP/6-31G* dihedral profiles of (a) unsubstituted and (b) model α-methylated analogue of 2.

desired, Phe19$_{(p53)}$-binding conformer (orange), destabilized by the adjacent p-chlorophenyl, is found to lie ~1 kcal/mol higher in energy than the anti global minimum (cyan). Disubstitution at the α-carbon effectively raises the energy of the undesired conformation, aiding equalization of the population (Figure 5b) and ensuring that one of the substituents will always be directed toward the p-chlorophenyl and into the Phe19$_{(p53)}$ pocket.

Compound 9, possessing an ethyl ester "directing group" at the α-position of the n-propyl substituent, was twice as potent as 5, while the other diastereomer, compound 10, was 2-fold less potent than 5 presumably because of the incorrect positioning of the ethyl group by the ester. Lengthening, shortening, or deleting the alkyl chain in 9 diminishes potency (11, 12, and 13). Notably, 9 was the only compound that showed measurable activity (IC$_{50}$ = 18.7 μM) in the biochemical assay upon addition of 15% human serum (Table 1).

Attention was then focused on optimizing the substituent at the C3 position (Table 2). Introduction of the (3R) acetic acid fragment to the piperidinone core of (5R,6S)-4 improved

Table 2. Modification of the Carboxylic Acid

Compd	R	HTRF IC$_{50}$ (μM)[a]	HTRF (15% HS[b]) IC$_{50}$ (μM)[a]
2	(CH$_2$COOH)	0.034 ± 0.006	0.37 ± 0.04
14	(CH$_2$COOH epimer)	0.076	1.11 ± 0.04
15	(vinyl)	6.5 ± 1.8	>30
16	(CH$_2$CH$_2$COOH)	0.57 ± 0.15	6.63 ± 0.53
17	(CH$_2$CH$_2$COOH epimer)	0.34 ± 0.03	6.64 ± 0.74
18	(CH$_2$COOMe)	0.79 ± 0.03	>30
19	(CH$_2$CONH$_2$)	0.27 ± 0.07	7.63 ± 0.98
20	(CH$_2$CN)	2.34 ± 0.06	>30
21	(CH$_2$-tetrazole)	0.014 ± 0.004	0.19 ± 0.02

[a]Potency data are reported as the average of at least two determinations. [b]HS = human serum.

potency in the biochemical assay by more than 20-fold, presumably because of the electrostatic interaction between the carboxylate anion and the H96 in MDM2 (IC$_{50}$ for **2** of 0.034 μM vs IC$_{50}$ for (5R,6S)-**4** of 0.82 μM). Compound **14**, the C3-epimer of **2**, was about 2-fold less potent than **2**. The length of the tether between the carboxylic acid and the piperidinone core in **2** appeared to be optimized, since the corresponding homologated acids lost potency (**16** and **17** vs **2** and **14**). Additional functional groups were evaluated for their ability to interact with H96. The terminal alkene (**15**) and nitrile (**20**) analogues were significantly less potent (over 70-fold). Hydrogen bond acceptors including ester (**18**) and amide (**19**) also had substantially reduced potency (over 10-fold). Only compound **21**, the tetrazole derivative with an acidic proton comparable to that of the carboxylic acid, exhibited slightly enhanced potency in the biochemical assay compared to **2**.

Having identified the key features for the *N*-alkyl group and the C3 position, an effort was made to synthesize a series of fully optimized derivatives and evaluate their activity in both biochemical and cell-based assays (Table 3). Two different cell-based assays, a functional p21 induction assay[16] and a proliferation assay[16] in the human osteosarcoma tumor cell line SJSA-1 (which displays MDM2 gene amplification), were employed. The cyclin-dependent kinase inhibitor, p21, is a direct transcription target of activated p53[23] and is involved in both cell cycle arrest[24] and apoptosis.[25,26] Induction of p21 is a proximal marker of p53 activity.[14,15]

Compound **22**, with an ethyl ester directing group on the *N*-alkyl fragment (Table 3), was 3−4 times more potent than **2** in the biochemical assay, the functional p21 induction assay, and the cell proliferation assay. The *tert*-butyl ester derivative **23** was even more potent than the ethyl ester **22**, with an additional 2-fold improvement in both biochemical and cell-based assays. Analogous to previous observations, replacement of the carboxylic acid in **23** with a tetrazole provided slightly enhanced potency (**24** vs **23**).

The X-ray crystal structure of compound **23** bound to human MDM2 was determined at a resolution of 1.8 Å (Figure 6)[27] and was found to be consistent with the proposed binding mode of **2** based on docking models. As predicted, the ethyl group occupies the Phe19$_{(p53)}$ binding pocket, with the *tert*-butyl ester directing group extending away from the protein with the carbonyl oxygen facing out toward solvent. Moreover, the *tert*-butyl group makes van der Waals contact with the surface of the MDM2 protein.

The X-ray cocrystal structure of **23** confirmed that the *trans*-C5 and C6 aryl groups reside in a *gauche*-like orientation when bound to MDM2. However, quantum mechanical calculations on the parent core structure (*N*-methyl, (*R*)-CH$_3$ at C3; Figure 7a) predict that in the free state, the more stable conformer instead possesses an *anti*-like arrangement of the C5 and C6 aryls (ΔE = 0.5 kcal/mol; B3LYP/6-31G*)[28] unsuitable for binding. Quaternization of the C3 position via disubstitution was predicted to stabilize the binding conformation, via a 1,3-steric interaction with the C5 aryl group when in the undesired, *anti* conformation (Figure 7b). The crystal structure of **23** bound to MDM2 shows that such substitution would project outward toward the solvent and not interfere with MDM2 binding. Quantum mechanical calculations predict a shift in the equilibrium from a calculated 1:3 ratio of binding to nonbinding conformer to one in which the binding, *gauche* form now dominates (>98%; ΔE = 2.4 kcal/mol).

Consistent with our hypothesis, it was found that substitution at C3 with a methyl group afforded compounds with increased potency. Compounds **25** and **26** were 2−3 times more potent in the biochemical and cellular assays than the corresponding C3 des-methyl compounds **23** and **24** (Table 4).

The ^{1}H NMR coupling constants of **25** and **23** at two different temperatures were also consistent with the theoretical predictions (Figure 8).[29] The vicinal coupling constant between the C5 and C6 methine protons (J_{ab}) of compound **23** at 298 and 203 K was 6.8 and 0 Hz, respectively. However J_{ab} for compound **25** was consistently 10.9 Hz at both temperatures. These results indicated that both *anti* and *gauche* conformations are present in **23** at 298 K, whereas only the *gauche* conformation exists for **25** at 298 K. At low temperature (203 K), the difference is even more significant. Compound **23** exists exclusively in the *anti* conformation, while the *gauche* conformation of **25** is still predominant.

Further in vitro assessment of these compounds revealed that the carboxylic acid **25** had less hPXR activation and CYP3A4 inhibition compared to tetrazole analogue **26** (Table 5). Compound **26**, the tetrazole version of **25**, had an unfavorable hPXR profile (65% activation at 2 μM) and inhibited CYP3A4 (80% inhibition at 3 μM). Compound **26** is also a strong time-

Table 3. Fully Functionalized Piperidinone Derivatives
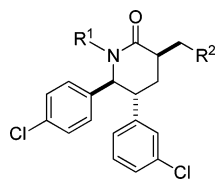
Compd	R[1]	R[2]	Biochemical Potency		Cellular Potency (SJSA-1)	
			HTRF IC$_{50}$ (nM)[a]	HTRF (15% HS[b]) IC$_{50}$ (nM)[a]	p21 (10% HS[b]) IC$_{50}$ (μM)[a]	EdU (10% HS[b]) IC$_{50}$ (μM)[a]
2	cyclopropyl	COOH	34.0 ± 5.8	372 ± 41	34.4 ± 3.4	3.35 ± 0.38
22	EtO$_2$C	COOH	7.6 ± 2.1	86 ± 17	10.7 ± 4.4	0.965 ± 0.046
23	t-BuO$_2$C	COOH	4.2 ± 0.9	43.3 ± 5.9	4.3 ± 0.7	0.476 ± 0.087
24	t-BuO$_2$C	tetrazole	1.8 ± 0.7	20.3 ± 3.5	3.1 ± 0.9	0.312 ± 0.091

[a]Potency data are reported as the average of at least two determinations. [b]HS = human serum.
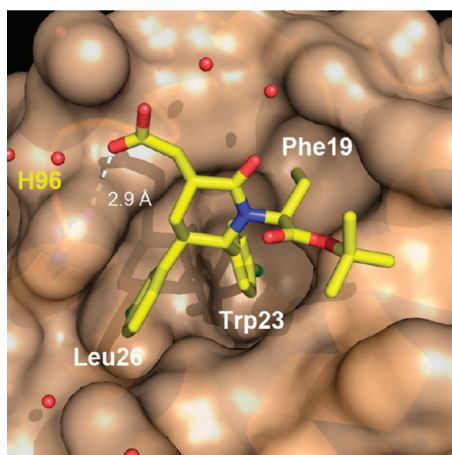
Figure 6. Co-crystal structure of **23** bound to human MDM2 (17−111) at 1.8 Å resolution. MDM2 binding pockets are labeled (by p53 side chain) in white, H96 labeled in yellow. Cocrystallized water molecules are shown in red.

dependent inhibitor of CYP3A4. In light of these data, compound **25** was selected for further evaluation.

To evaluate its selectivity, we examined the effect of **25** on inhibiting the proliferation of HCT116 p53^{wt} and p53$^{−/−}$ tumor cells in vitro.[16] HCT116 p53^{wt} and p53$^{−/−}$ tumor cells were incubated with **25** for 16 h, and the percentage of cell-growth inhibition was measured in a BrdU proliferation assay. Potency in wild-type p53 cells (IC$_{50}$ = 0.85 ± 0.23 μM) was substantially higher than that in p53 deficient cells (IC$_{50}$ > 25 μM) (Figure 9a). Similarly, compound **25** also exhibited a dose-dependent increase of p21 mRNA in HCT116 p53^{wt} cells (IC$_{50}$ = 1.0 ± 0.5 μM) in the p21 induction assay. In contrast, no

effect on p21 mRNA was observed when **25** was treated with HCT116 p53$^{−/−}$ tumor cell lines for 7 h (Figure 9b).

A pharmacodynamic (PD) study[30] with **25** in the SJSA-1 tumor xenograft model was also completed. SJSA-1 tumor cells
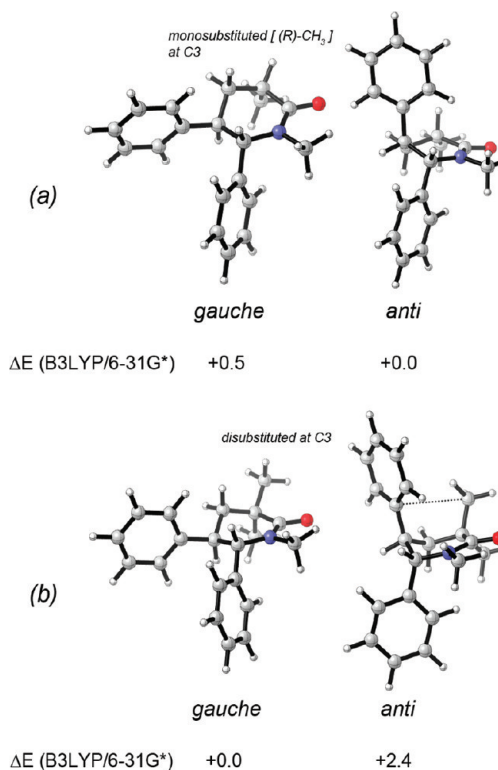
Figure 7. B3LYP/6-31G* structures and relative energies (kcal/mol) for (a) C3 (*R*)-monosubstituted and (b) C3-disubstituted systems.

Table 4. C3 Me Piperidinone Derivatives
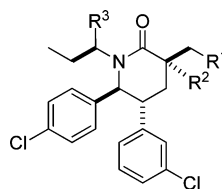
Compd	R[1]	R[2]	R[3]	Biochemical Potency		Cellular Potency (SJSA-1)	
				HTRF IC$_{50}$ (nM)[a]	HTRF (15% HS[b]) IC$_{50}$ (nM)[a]	p21 (10% HS[b]) IC$_{50}$ (µM)[a]	EdU (10% HS[b]) IC$_{50}$ (µM)[a]
23	COOH	H	O-tBu carbamate	4.2 ± 0.9	43.3 ± 5.9	4.3 ± 0.7	0.48 ± 0.09
24	tetrazole	H	O-tBu carbamate	1.8 ± 0.7	20.3 ± 3.5	3.1 ± 0.9	0.31 ± 0.09
25	COOH	Me	O-tBu carbamate	2.2 ± 0.7	19.9 ± 7.5	1.9 ± 0.5	0.19 ± 0.06
26	tetrazole	Me	O-tBu carbamate	0.90 ± 0.21	9.0 ± 2.7	1.6 ± 0.7	0.17 ± 0.03
27	COOH	Me	propyl	2.8 ± 0.2	36.3 ± 6.7	5.5 ± 1.2	0.54 ± 0.08
28	COOH	Me	HO-ethyl	1.7 ± 0.2	6.8 ± 2.4	1.5 ± 0.5	0.21 ± 0.06
29	COOH	Me	HO-isopropyl	1.1 ± 0.5	4.2 ± 1.8	0.76 ± 0.29	0.068 ± 0.016
Nutlin-3a	N/A	N/A	N/A	17.8 ± 4.2	89 ± 12	7.1 ± 1.7	0.70 ± 0.23

[a]Potency data are reported as the average of at least two determinations. [b]HS = human serum.
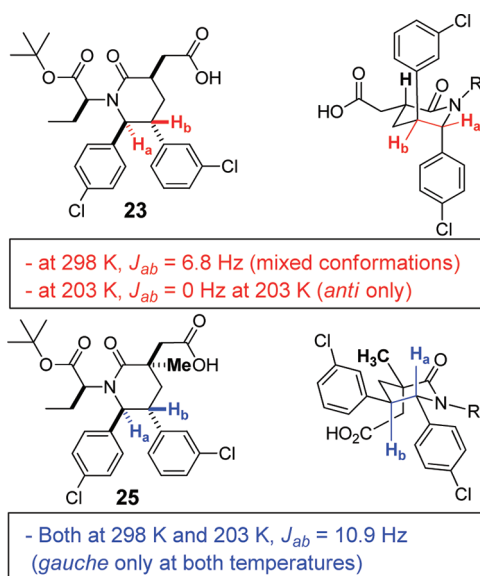
Figure 8. Vicinal coupling constant between C5 and C6 methine protons (J_{ab}) in compounds **23** and **25** at two different temperatures, 298 and 203 K. ^{1}H proton NMR spectra were obtained in MeOH-d_4.

Table 5. Comparison of 25 and 26 in Selected PKDM Assays

	25	26
hPXR activation, % of control[a] at 2 µM	27	65
CYP3A4, % inhibition at 3 µM	40	80
TDI, % remaining of CYP3A4 over control[b] after 15 min at 10 µM	77	30

[a]Rifampin used as a positive control. [b]DMSO used as a control.

were implanted in the mice 2 weeks prior to treatment. Compound **25** was administered orally, and p21 mRNA induction levels were measured. In this experiment, peak induction of p21 was observed approximately 6 h after dosing (15-fold induction at 300 mg/kg) (Figure 10a). In a parallel experiment, a dose-dependent increase in p21 mRNA induction (6 h) was also observed (Figure 10b).

Next, the ability of **25** to inhibit tumor growth in the SJSA-1 xenograft model was evaluated.[30] After a 12-day incubation of SJSA-1 human cancer cells in the mice, compound **25** was orally administered once daily for 14 days, and the tumor volume was monitored. Treatment with **25** showed a dose-dependent inhibition of tumor growth with a calculated ED$_{50}$ of 118 mg/kg. At 200 mg/kg, 91% tumor growth inhibition was observed (Figure 11).

(a) Proliferation (BrdU, 16 hr)   (b) p21 Induction (7 hr)

Figure 9. The cell activity of **25** is p53 dependent. (a) In HCT116 p53[wt] and p53^{−/−} cells, the percentage of BrdU positive cells was measured 16 h after compound treatment by flow cytometry. DMS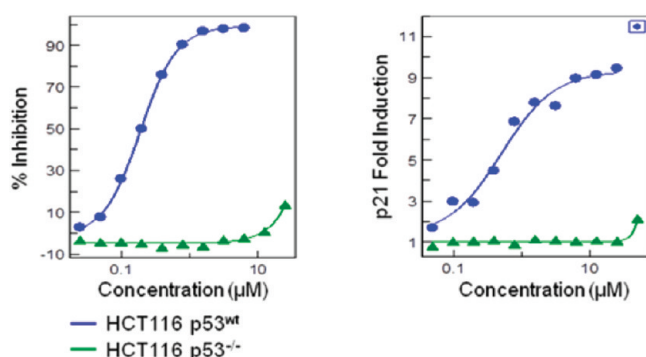O control was designated as 0% inhibition. (b) In HCT116 p53[wt] and p53^{−/−} cells, total RNA was extracted 7 h after compound treatment and p21 mRNA was measured by quantitative RT-PCR.

The demonstration of robust antitumor efficacy in xenograft studies with compound **25** led us to focus on further optimization to improve potency and pharmacokinetic (PK) properties. On the basis of the X-ray cocrystal structure of **23** with the MDM2 protein (Figure 6), in which the carbonyl of the *tert*-butyl ester points away from the protein, it was hypothesized that replacing the *tert*-butyl ester with other functional groups would allow us to modulate the physicochemical properties of our molecules without disrupting critical interactions with the protein. Although the *tert*-butyl group does engage in some degree of van der Waals contact with the protein, we felt that such modification could also potentially offer an opportunity to enhance potency by picking up better interactions with the protein surface than those provided by the *tert*-butyl ester.

A variety of functional groups such as alcohols, amides, amines, and heterocycles are tolerated in this area of the molecule (Figure 12). These changes provided diverse physicochemical properties while maintaining acceptable potency.[31] For example, replacing the *tert*-butyl ester in **25** with an ethyl group (**27**) or a primary alcohol (**28**) provided molecules with good biochemical potency (IC$_{50}$ for **27** of 2.8 nM and IC$_{50}$ for **28** of 1.7 nM in Table 4), although the ethyl derivative (**27**) showed a greater loss in potency upon addition of human serum compared to the primary alcohol (IC$_{50}$ for **27** of 36.3 nM vs IC$_{50}$ for **28** of 6.8 nM). Relative to **28**, compound **27** also exhibited a higher IC$_{50}$ in cell-based assays, apparently because of the protein binding differences. Interestingly, addition of a methyl group to the α-position of the hydroxyl group in **28** boosted potency 2- to 3-fold in the biochemical and cell-base assays (**29** vs **28**). On the basis of its potency, pharmacokinetic properties, and selectivity, the secondary alcohol derivative **29** was selected for further development.

The dissociation constant (K_D) for **29** and **25** was determined in a surface plasmon resonance (SPR) spectroscopy binding assay (Table 6).[16] The K_D of **29** was 0.4 nM, while that of **25** was 1.0 nM. Compound **29** is consistently more potent than **25** in the biochemical and cell-based assays. Evaluation of **29** in the HCT116 p53[wt] and HCT116 p53^{−/−} tumor cell lines showed >100-fold selectivity and is consistent with the data

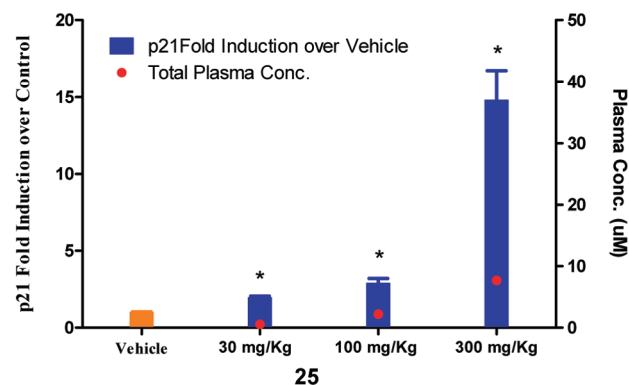(a) Time Course
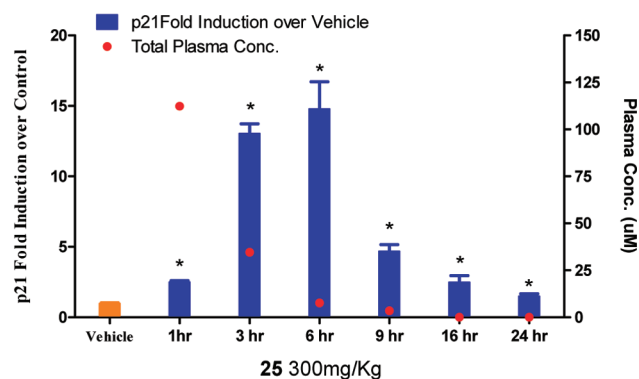
(b) Dose Response (6 hr)

Figure 10. PD study results of compound **25** in SJSA1 tumor xenograft: *$p < 0.05$. Female athymic nude mice were implanted subcutaneously with 5×10^6 SJSA-1 cells. When tumors reached ~175 mm^3, (a) **25** or vehicle was administered orally once. Mice were sacrificed at 1, 3, 6, 9, 16, and 24 h postdose ($n = 5$/group). (b) Vehicle or 30, 100, or 300 mg/kg **25** was administered orally once. Mice were sacrificed at 6 h postdose ($n = 5$/group). Tumors were immediately removed and snap-frozen. p21 mRNA levels were measured by quantitative RT-PCR. Tumors treated with vehicle served as a negative control and indicated the baseline p21 mRNA level. Data are represented as mean p21 fold induction over vehicle, and error bars represent SEM of data from five mice. Concentrations in blood plasma were analyzed by LC/MS/MS.

observed with **25**. It was also found that **29** had reduced liability in the hPXR, CYP3A4, and TDI assays compared to **25**. In addition to its suitable pharmacokinetic profile in rat, **29** exhibited low plasma clearance relative to hepatic blood flow in cynomolgus monkey (CL = 0.72 L h^{-1} kg^{-1}) with a high volume of distribution (6.2 L/kg) and long half-life ($t_{1/2}$ = 14 h).

The most significant advantage of **29** over **25** is its greatly improved human hepatocyte intrinsic clearance (3.0 μL/min per 10^6 cells for **29** vs 26 μL/min per 10^6 cells for **25**), which resulted in extended predicted human half-life (>12 h for **29** vs 0.28 h for **25**). Given the improved potency and superior predicted human PK properties of **29**, we decided to evaluate its pharmacodynamic response and ability to inhibit tumor growth in the SJSA-1 mouse xenograft model.

The effect of **29** on p21 mRNA induction after dosing q.d. for 4 days at 150 mg/kg was evaluated in the mouse SJSA-1 tumor model. As shown in Figure 13, **29** caused significant and time-dependent p21 induction over vehicle. A 14-fold induction
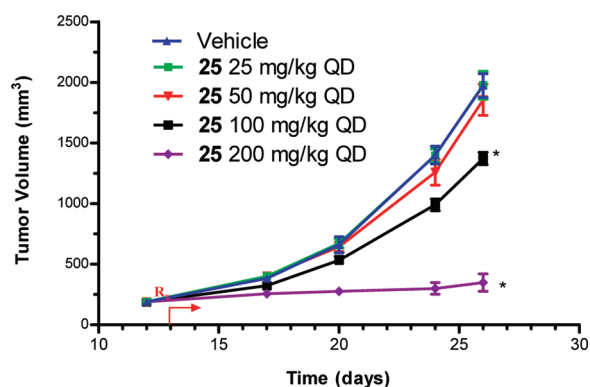
Figure 11. Inhibition of SJSA-1 tumor xenograft growth by compound 25: *$p < 0.05$. SJSA-1 cells (5×10^6) were implanted subcutaneously into female athymic nude mice. Treatment with vehicle or 25 at 25, 50, 100, or 200 mg/kg q.d. by oral gavage began on day 12 when tumors had reached ~200 mm³ ($n = 10$/group). Tumor sizes and body weights were measured twice per week. Data are represented as mean tumor volumes, and the error bars represent SEM of data from 10 mice.
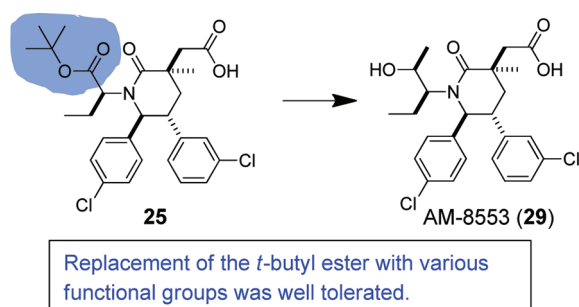

Replacement of the *t*-butyl ester with various functional groups was well tolerated.

Figure 12. Transformation of 25 into 29.

Table 6. Comparison of 25 and 29

	25	29
Biochemical Potency		
K_D (SPR, nM)	1.0	0.4
IC_{50} (HTRF, nM)	2.2 ± 0.7	1.1 ± 0.5
IC_{50} [a] (HTRF, nM)	19.9 ± 7.5	4.2 ± 1.8
Cellular Potency (SJSA-1)		
p21 IC_{50} [b] (μM)	1.9 ± 0.5	0.76 ± 0.29
EdU IC_{50} [b] (μM)	0.19 ± 0.06	0.068 ± 0.016
Specificity (HCT116)		
BrdU IC_{50} [b] (p53^{wt}, μM)	0.85 ± 0.23	0.20 ± 0.12
BrdU IC_{50} [b] (p53$^{-/-}$, μM)	>25	>25
hPXR Activation		
% of control[c] at 2 μM	27	15
CYP3A4		
% inhibition at 3 μM	40	13
TDI		
% remaining of CYP3A4 over control[d] after 15 min at 10 μM	77	96
Rat PK		
CL (L h^{-1} kg^{-1})	2.7	1.2
V_{dss} (L/kg)	1.5	12
F (%)	77	100
Mouse PK		
CL (L h^{-1} kg^{-1})	1.5	3.5
V_{dss} (L/kg)	1.3	5.2
F (%)	36	12
Hepatocyte Stability		
human (μL/min per 10^6 cells)	26	3.0
Projected Human PK		
CL (L h^{-1} kg^{-1})	0.55	0.03
half-life (h)	0.28	>12

[a]15% human serum. [b]10% human serum. [c]Rifampin used as a positive control. [d]DMSO used as a control.

of p21 mRNA was observed 4 h postdose. The AUC of p21 fold induction was about 2-fold greater than that observed with 25 at 300 mg/kg q.d. dosing (230-fold p21 induction·h/day for 29 vs 135-fold p21 induction·h/day for 25). Furthermore, 29 also demonstrated a dose-dependent effect on p21 mRNA induction in SJSA-1 tumors (data not shown).

Compound 29 was also evaluated for its ability to inhibit tumor growth in the SJSA-1 mouse xenograft model. As expected, a dose-dependent response of tumor growth inhibition was observed with 29. It significantly inhibited tumor growth at 150 and 200 mg/kg q.d. compared to vehicle, with an ED$_{50}$ of 78 mg/kg (Figure 14). Importantly, 200 mg/kg q.d. of 29 caused tumor regression ($R = 27\%$). There was no body weight loss in any of the treatment groups.

Since 29 has a relatively high clearance (CL = 3.5 L h^{-1} kg^{-1}) and short half-life time ($t_{1/2}$ = 2.6 h) in mouse, we decided to explore whether more frequent dosing of 29 would lead to enhanced tumor growth inhibition in the SJSA-1 xenograft model. A b.i.d. treatment caused a dose-dependent reduction in tumor growth with statistically significant inhibition at 75 and 100 mg/kg compared to vehicle (Figure 15). Overall, inhibition with b.i.d. dosing was comparable to that of q.d. dosing at all dose levels. Again, no significant body weight loss was observed for any of the treated groups compared to the vehicle group.

Finally, the cocrystal structure of 29 with human MDM2 protein was obtained by X-ray crystallography to a resolution of 2.0 Å (Figure 16).[32] As was seen with the structure of 23, compound 29 occupies the three critical binding pockets. The

C5 aryl group fills the Leu26$_{(p53)}$ pocket and engages in a face-to-face, π-stacking interaction with H96, while the C6 aryl group occupies the Trp23$_{(p53)}$ binding cavity. The hydroxyl
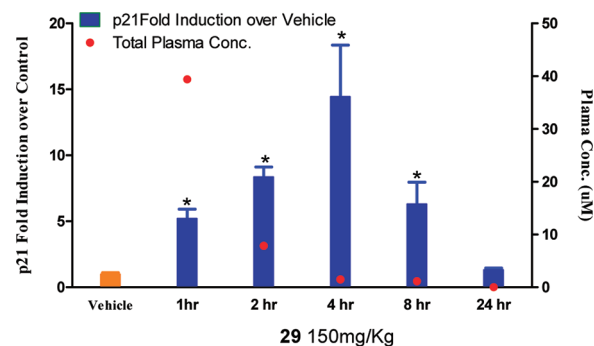
Figure 13. PD study results of compound 29 in SJSA-1 tumor xenograft: *$p < 0.05$. Female athymic nude mice were implanted subcutaneously with 5×10^6 SJSA-1 cells. When tumors reached ~175 mm³, 29 or vehicle was administered orally once daily (q.d.) for 4 days. Mice were sacrificed on day 4 at 1, 2, 4, 8, and 24 h postdose ($n = 5$/group). Tumors were immediately removed and snap-frozen. p21 mRNA levels were measured by quantitative RT-PCR. Tumors treated with vehicle served as a negative control and indicated the baseline p21 mRNA level. Data are represented as mean p21 fold induction over vehicle, and error bars represent SEM of data from five mice. Concentrations in blood plasma were analyzed by LC/MS/MS.
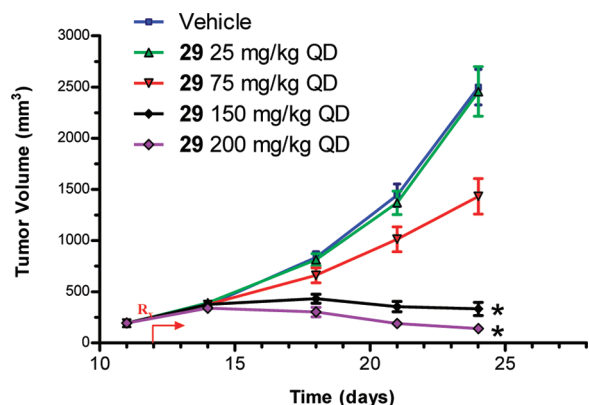
Figure 14. Inhibition of SJSA1 tumor xenograft growth by **29**: *$p < 0.05$. SJSA-1 cells (5×10^6) were implanted subcutaneously into female athymic nude mice. Treatment with vehicle or **29** at 25, 75, 150, or 200 mg/kg q.d. by oral gavage began on day 11 when tumors had reached ~200 mm^3 ($n = 10$/group). Tumor sizes and body weights were measured twice per week. Data are represented as mean tumor volumes, and the error bars represent SEM of data from 10 mice.

Figure 15. SJSA-1 cells (5×10^6) were implanted subcutaneously into female athymic nude mice: *$p < 0.05$. Treatment with vehicle or **29** at 25, 50, 75, or 100 mg/kg b.i.d. by oral gavage began on day 10 when tumors had reached ~200 mm^3 ($n = 10$/group). Tumor sizes and body weights were measured twice per week. Data are represented as mean tumor volumes, and the error bars represent SEM of data from 10 mice.

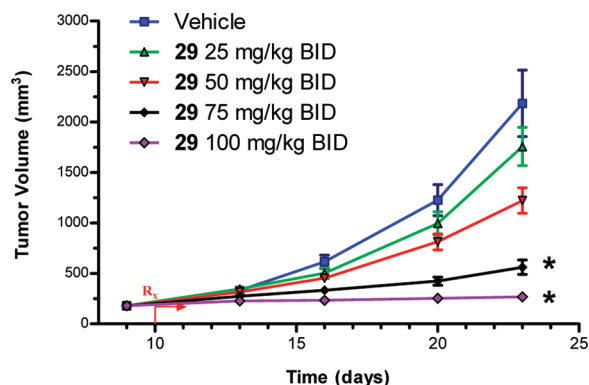group is exposed to solvent and the ethyl group directed into the Phe19$_{(p53)}$ pocket by the conformational constraint induced by the α-substitution. Additionally, the carboxylate of **29** interacts with adjacent and presumably charged imidazole on the H96 side chain of MDM2. Finally, this cocrystal structure shows that the C3 methyl group points directly out toward solvent, supporting our proposal that the potency increase from C3 methylation (**23** vs **25**) is conformationally induced and independent of protein contacts.

■ CHEMISTRY

The synthesis of *cis*-piperidinone **1** started with the preparation of ketone **31**, which was obtained from the reaction of the dianion of 2-(3-chlorophenyl)acetic acid (**30**) with methyl 4-chlorobenzoate. Subsequent conjugate addition with methyl acrylate, followed by reduction with NaBH$_4$ provided alcohol **32** as a single diastereomer. Bromination of **32** with CBr$_4$ and PPh$_3$, followed by displacement with NaN$_3$, gave azide **33**. The piperidinone core **34** was obtained from the Staudinger
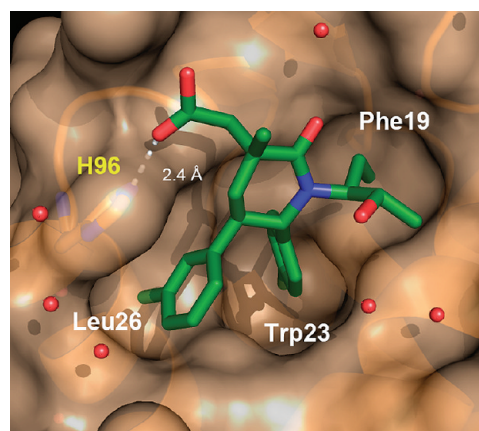
Figure 16. Cocrystal structure of **29** bound to human MDM2 (17−111) at 2.0 Å resolution. White labels indicate the positions normally occupied by key p53 residues. H96 is labeled in yellow. Cocrystallized water molecules are shown in red.

reaction of azide with Me$_3$P, followed by cyclization under mildly basic conditions. Deprotonation of **34** with NaH and treatment with cyclopropylmethyl bromide provided intermediate **35**, which was alkylated at C3 with NaHMDS and allyl bromide (dr = 99:1). Oxidative cleavage of the alkene in **36** with catalytic ruthenium tetroxide provided the desired racemic piperidinone acid **1** (Scheme 1).

Compounds **3−13** were synthesized according to the procedures outlined in Scheme 2. The preparation of the racemic piperidinone core **3** started with mesylation of **32**, followed by displacement with NaN$_3$, to provide azide **37**. The piperidinone core **3** was obtained via procedures similar to those described for the synthesis of **34**. Alkylation of **3** with the

Scheme 1[a]
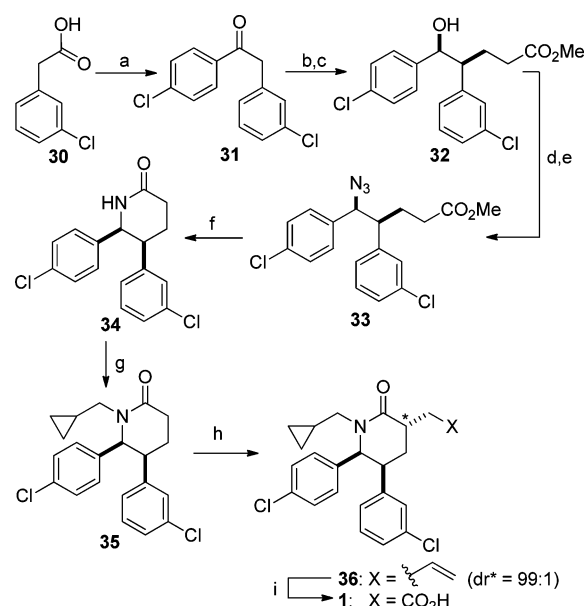
[a]Reagents and conditions: (a) NaHMDS, 4-ClPhCO$_2$Me, THF, 50%; (b) methyl acrylate, *t*-BuOK, THF, 84%; (c) NaBH$_4$, MeOH, 82%; (d) CBr$_4$, PPh$_3$, DCM, 80%; (e) NaN$_3$, DMF, 77%; (f) Me$_3$P, THF/H$_2$O; NaHCO$_3$, MeOH/H$_2$O, 87%; (g) cyclopropylmethyl bromide, NaH, THF, 84%; (h) LiHMDS, allyl bromide, 84%; (i) RuCl$_3$, NaIO$_4$, CH$_3$CN/CCl$_4$/H$_2$O, 79%.

Scheme 2[a]
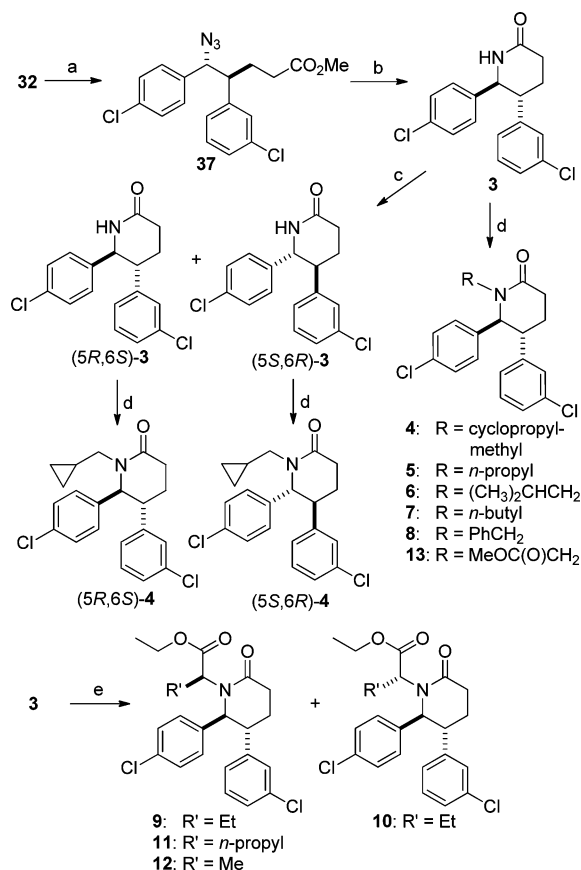
[a]Reagents and conditions: (a) MsCl, TEA, DCM; NaN₃, DMF, 56%; (b) Me₃P, THF/H₂O; NaHCO₃, MeOH/H₂O, 88%; (c) separation by chiral HPLC; (d) primary alkyl halide, NaH, DMF, 70–90%; (e) EtOC(O)CHBrR′, NaH, DMF, 75–83%.

corresponding primary alkyl halides provided **4–8** and **13**. Compounds **9–12** were prepared by N-alkylation of **3** with EtOC(O)-CHBrR′, followed by separation of diastereomers using silica gel column chromatography (R′ = Me, dr = 2.3:1; R′ = Et, dr = 1.8:1; R′ = n-Pr, dr = 1:1 in favor of the desired S-isomer). Preparation of (5R,6S)-**4**[33] and (5S,6R)-**4**[33] was accomplished by separation of the enantiomers in **3** using normal phase chiral HPLC, followed by N-alkylation of each enantiomer.

Scheme 3 describes the synthesis of compounds **2** and **14–21**. C3 allylation of (5R,6S)-**4**, followed by separation of diastereomers gave **15**[34] and its C3 epimer, **38**.[34] Oxidative cleavage of the alkene in **15** and **38** with catalytic ruthenium tetroxide provided acid **2** and its C3 epimer **14**, respectively. In a similar manner, the homologated acids **16** and **17** were synthesized from homoallyl intermediates **39**[34] and **40**.[34] Compound **2** was converted to its methyl ester **18** by SOCl₂/MeOH. Direct transformation of ester **18** to primary amide **19** was achieved using 7 M NH₃ in MeOH. Dehydration of **19** with trifluoroacetic acid anhydride and TEA provided nitrile **20**, which was converted to the tetrazole **21** using sodium azide.

Compounds **22–24**[33] were synthesized in a straightforward manner, through the routes illustrated in Scheme 4. After N-alkylation of (5R,6S)-**3** with ROC(O)CHBrEt, the desired S-isomer was isolated by silica gel column chromatography (R = Et, dr = 1.8:1; R = t-Bu, dr = 4.6:1 in favor of the S-isomer) and

Scheme 3[a]
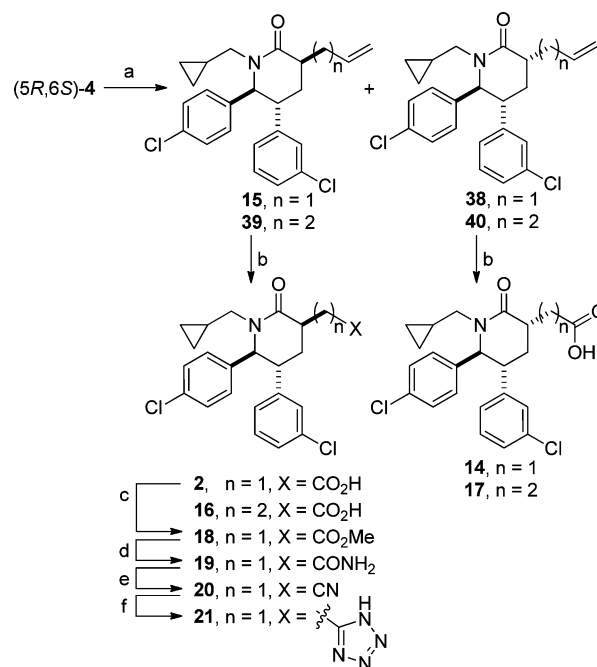
[a]Reagents and conditions: (a) for n = 1, allyl bromide, LiHMDS, THF, 85%; for n = 2, 4-bromo-1-butene, LiHMDS, THF, 42%; (b) NaIO₄, RuCl₃, CH₃CN/CCl₄/H₂O, 70–82%; (c) SOCl₂, MeOH, 89%; (d) 7 M NH₃, in MeOH, 78%; (e) (CF₃CO)₂O, TEA, THF, 93%; (f) NaN₃, NH₄Cl, DMF, 90 °C, 41%.

Scheme 4[a]
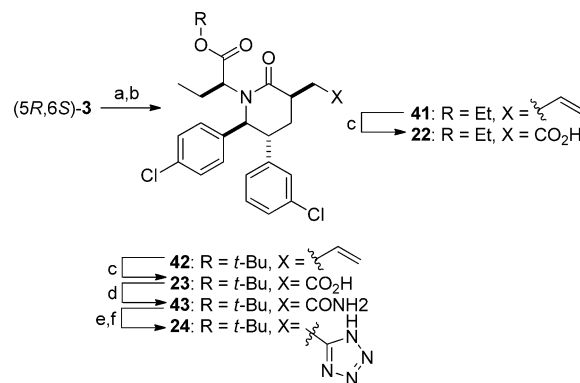
[a]Reagents and conditions: (a) ROC(O)CHBrEt, NaH, DMF, 42–46%; (b) allyl bromide, LiHMDS, THF, 75–80%; (c) NaIO₄, RuCl₃, CH₃CN/CCl₄/H₂O, 60–70%; (d) isobutyl chloroformate, N-methyl-morpholinone, NH₄OH, 90%; (e) (CF₃CO)₂O, TEA, THF, 85%; (f) NaN₃, NH₄Cl, DMF, 90 °C, 45%.

was subjected to C3 allylation to provide a mixture of two C3 isomers (R = Et, dr = 1.6:1; R = t-Bu, dr = 4.9:1 in favor of the S-isomer). Again, the desired S-isomer was isolated by silica gel column chromatography (**41**, R = Et; **42**, R = t-Bu) and treated with NaIO₄ and RuCl₃ to afford acids **22** and **23**. Further modification of the carboxylic acid in **23** into the tetrazole via amide coupling with NH₃ (**43**), dehydration, and reaction with sodium azide yielded **24**.

Compounds **25–29**[33] were synthesized via the routes outlined in Scheme 5. Introduction of a DMB (2,4-dimethoxybenzyl) protecting group to the amide nitrogen of (5R,6S)-**3** with freshly prepared DMBCl[35] followed by

Scheme 5[a]
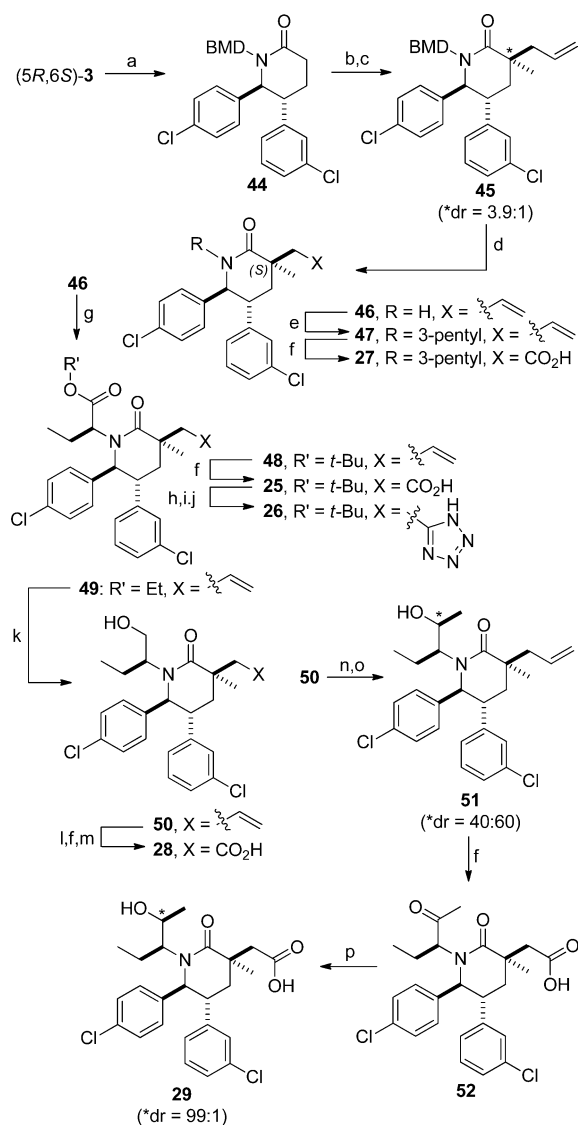
*a*Reagents and conditions: (a) DMBCl, NaH, 25 °C, 85%; (b) MeI, LiHMDS, THF, −78 °C, 91%; (c) allyl bromide, LiHMDS, THF, 40 °C 82%; (d) TFA, 50 °C, 70%; (e) 3-bromopentane, NaH, 40%; (f) NaIO$_4$, RuCl$_3$, CH$_3$CN/CCl$_4$/H$_2$O, 47−80%; (g) R′OC(O)CHBrEt, NaH, DMF, 40−50%; (h) isobutyl chloroformate, N-methylmorpholinone, NH$_4$OH, 90%; (i) (CF$_3$CO)$_2$O, TEA, THF, 80%; (j) NaN$_3$, NH$_4$Cl, DMF, 90 °C, 41%; (k) LiBH$_4$, Et$_2$O, 75%; (l) TBDPSCl, imidazole, 90%; (m) TBAF, 78%; (n) Dess−Martin periodinane, 79%; (o) MeMgBr, THF, 87%; (p) L-Selectride, −78 °C, 80%.

sequential methylation and allylation of the DMB protected core (**44**) gave **45** with the desired C3-epimer as a major product (dr = 3.9:1 in favor of the S-isomer). Removal of the DMB group using TFA and separation of the diastereomers by silica gel column chromatography provided **46**. The 3-pentyl derivative **27** was synthesized by N-alkylation of **46** with neat 3-bromopentane and NaH, followed by the reaction of **47** with NaIO$_4$ and RuCl$_3$, as before. N-Alkylation of **46** with R′OC(O)-CHBrEt followed by isolation of the desired isomer by silica gel column chromatography afforded intermediates **48** (R′ = t-Bu) and **49** (R′ = Et) (R′ = t-Bu, dr = 2.2:1; R′ = Et, dr = 1:1 in favor of the desired S-isomer). The carboxylic acid (**25**) and the tetrazole (**26**) were prepared from **48** via procedures

similar to those described for the synthesis of **23** and **24**. Reduction of **49** with LiBH$_4$ in Et$_2$O provided the primary alcohol **50** which was oxidized with Dess−Martin periodinane. The resulting aldehyde was treated with MeMgBr to give the secondary alcohol **51** as a mixture of two diastereomers (dr = 40:60 in favor of the R-isomer). Simultaneous oxidation of both the secondary alcohol and the alkene in **51** with ruthenium tetroxide provided keto acid **52** in good yield. Finally, reduction of methyl ketone **52** with L-Selectride at −78 °C gave **29** as the predominant product (dr = 99:1 in favor of the S-isomer).[36]

■ CONCLUSION

In summary, the synthesis and initial SAR of rigid cores capable of holding two aromatic rings in proximity led to the identification of **1** as a novel inhibitor of the MDM2−p53 protein−protein interaction. Optimization of **1** led to the discovery of **2**, a piperidinone derivative featuring an acetic acid substituent at C3 capable of forming an electrostatic interaction with the H96 imidazole side chain of MDM2. Systematic optimization of the N-alkyl substituent of **2** led to molecules with highly populated, well-defined free-state conformations suited for optimal binding. These molecules were designed to occupy the Phe19 pocket, provide polar functional groups to interact with solvent, and gain additional van der Waals contact with the MDM2 protein. In addition, optimization of the piperidinone ring led to stabilization of the desired trans-diaryl conformation of these molecules by incorporation of a methyl group at the C3 position, leading to the discovery of **25**.

Further optimization resulted in the discovery of **29** which demonstrated superior efficacy in 14-day SJSA-1 xenograft studies. Compound **29** is a highly potent, selective, and orally bioavailable inhibitor of the MDM2−p53 interaction and is projected to have low clearance and a long half-life in humans.

■ EXPERIMENTAL SECTION

General Chemistry. All reactions were conducted under an inert gas atmosphere (nitrogen or argon) using a Teflon-coated magnetic stir bar at the temperature indicated. Commercial reagents and anhydrous solvents were used without further purification. Analytical thin layer chromatography (TLC) and flash chromatography were performed on Merck silica gel 60 (230−400 mesh). Removal of solvents was conducted by using a rotary evaporator, and residual solvent was removed from nonvolatile compounds using a vacuum manifold maintained at approximately 1 Torr. All yields reported are isolated yields. Preparative reversed-phase high pressure liquid chromatography (RP-HPLC) was performed using an Agilent 1100 series HPLC and Phenomenex Gemini C18 column (5 μm, 100 mm × 30 mm i.d.), eluting with a binary solvent system A and B using a gradient elusion [A, H$_2$O with 0.1% trifluoroacetic acid (TFA); B, CH$_3$CN with 0.1% TFA] with UV detection at 220 nm. All final compounds were purified to ≥95% purity as determined by an Agilent 1100 series HPLC with UV detection at 220 nm using the following method: Zorbax SB-C8 column (3.5 μm, 150 mm × 4.6 mm i.d.); mobile phase, A = H$_2$O with 0.1% TFA, B = CH$_3$CN with 0.1% TFA; gradient, 5−95% B (0.0−15.0 min); flow rate, 1.5 mL/min. Low-resolution mass spectral data were determined on an Agilent 1100 series LCMS with UV detection at 254 nm and a low resolution electrospray mode (ESI). High-resolution mass spectra were obtained on an Agilent 6510 Q-TOF MS instrument with an Agilent 1200 LC on the front end. ^{1}H NMR spectra were obtained on a Bruker Avance III 500 (500 MHz) or Bruker Avance II 400 (400 MHz) spectrometer. Chemical shifts (δ) are reported in parts per million (ppm) relative to residual undeuterated solvent as an internal reference. The following abbreviations were used to explain the multiplicities: s = single; d = doublet, t = triplet, q = quartet, dd = doublet of doublets, dt = doublet of triplets, m = multiplet, br = broad. Optical rotations ([α]$_D$) were

measured on a JASCO P-1020 polarimeter. Specific rotations are given as deg/dm, and the concentrations are reported as g/100 mL of the specific solvent and were recorded at the temperature indicated.

2-(3-Chlorophenyl)-1-(4-chlorophenyl)ethanone (31). To a solution of **30** (13.0 g, 76.0 mmol) in THF (250 mL) was added NaHMDS (1.0 M in THF, 160 mL, 160 mmol) slowly over 15 min at −78 °C. After the mixture was stirred at −78 °C for 20 min, a solution of methyl 4-chlorobenzoate (13.0 g, 76.0 mmol) in THF (50 mL) was added over 10 min. The resulting solution was allowed to warm to 25 °C and stirred for 2 h. The reaction was quenched (ice-cold water) and extracted (2 × EtOAc). The combined organic layers were dried (Na$_2$SO$_4$) and concentrated under reduced pressure. Flash column chromatography (SiO$_2$, 5−7% EtOAc/hexanes, gradient elution) provided **31** (10.2 g, 50% yield) as a white solid: ^{1}H NMR (400 MHz, CDCl$_3$) δ ppm 7.93−7.96 (2 H, m), 7.42−7.48 (2 H, m), 7.23−7.30 (3 H, m), 7.12−7.16 (1 H, m), 4.24 (2 H, s); MS (ESI) 265.0 [M + H][+].

(±)-(4S,5S)-Methyl 4-(3-Chlorophenyl)-5-(4-chlorophenyl)-5-hydroxypentanoate (32). To a solution of **31** (5.62 g, 21.2 mmol) and methyl acrylate (1.91 mL, 21.2 mmol) in THF (60 mL) was added t-BuOK (1.0 M in THF, 2.12 mL, 2.12 mmol) at 0 °C, and the mixture was allowed to warm to 25 °C. After being stirred at 25 °C for 1 h, the mixture was concentrated under reduced pressure, diluted (H$_2$O), extracted (2 × EtOAc), and washed (brine). The combined organic layers were dried (Na$_2$SO$_4$) and concentrated under reduced pressure. Flash column chromatography (SiO$_2$, 10% EtOAc/hexanes) provided methyl 4-(3-chlorophenyl)-5-(4-chlorophenyl)-5-oxopentanoate (6.23 g, 84% yield) as a colorless liquid: ^{1}H NMR (500 MHz, CDCl$_3$) δ ppm 7.87−7.90 (2 H, m), 7.37−7.41 (2 H, m), 7.26−7.28 (1 H, m), 7.20−7.26 (2 H, m), 7.14−7.17 (1 H, m), 4.64 (1 H, t, J = 7.3 Hz), 3.67 (3 H, s), 2.40−2.48 (1 H, m), 2.31 (2 H, t, J = 7.2 Hz), 2.09−2.19 (1 H, m); MS (ESI) 351.1 [M + H][+].

To a solution of the product above (6.23 g, 17.8 mmol) in MeOH (60 mL) was added NaBH$_4$ (671 mg, 17.7 mmol) at 0 °C. After the mixture was stirred at 25 °C for 1 h, the reaction was quenched (ice-cold H$_2$O) and extracted (2 × EtOAc). The combined organic layers were washed (brine), dried (Na$_2$SO$_4$), and concentrated under reduced pressure. Flash column chromatography (SiO$_2$, 20−30% EtOAc/hexanes, gradient elution) provided **32** (5.14 g, 82% yield) as a colorless liquid: ^{1}H NMR (400 MHz, CDCl$_3$) δ ppm 7.29−7.34 (2 H, m), 7.25−7.27 (2 H, m), 7.19−7.24 (3 H, m), 7.03−7.07 (1 H, m), 4.76 (1 H, d, J = 7.4 Hz), 3.58 (3 H, s), 2.81−2.88 (1 H, m), 2.00−2.13 (2 H, m), 1.74−1.96 (2 H, m); MS (ESI) 375.1 [M + Na][+].

(±)-(4S,5S)-Methyl 5-Azido-4-(3-chlorophenyl)-5-(4-chlorophenyl)pentanoate (33). To a solution of **32** (300 mg, 0.849 mmol) in DCM (5 mL) were added carbon tetrabromide (422 mg, 1.27 mmol) and triphenylphosphine (334 mg, 1.27 mmol) sequentially at 0 °C. After the mixture was stirred at 0 °C for 3 h, the reaction was quenched (ice-cold H$_2$O) and extracted (2 × DCM). The combined organic layers were washed (brine), dried (Na$_2$SO$_4$), and concentrated under reduced pressure. Flash chromatography (SiO$_2$, 10−15% EtOAc/hexanes, gradient elution) provided (±)-(4S,5R)-methyl 5-bromo-4-(3-chlorophenyl)-5-(4-chlorophenyl)pentanoate (283 mg, 80% yield) as a colorless liquid: ^{1}H NMR (500 MHz, CDCl$_3$) δ ppm 7.13−7.18 (2 H, m), 7.08−7.13 (4 H, m), 6.94−6.99 (1 H, m), 6.79−6.86 (1 H, m), 5.02 (1 H, d, J = 10.0 Hz), 3.64 (2 H, s), 3.13−3.37 (1 H, m), 2.70−2.89 (1 H, m), 2.11−2.22 (2 H, m), 1.91−2.05 (1 H, m).

To a solution of the bromide above (280 mg, 0.673 mmol) in DMF (1.8 mL) was added NaN$_3$ (219 mg, 3.36 mmol). After being stirred at 100 °C for 30 min, the mixture was cooled to ambient temperature, diluted (water), extracted (2 × EtOAc), and washed (3 × brine). The combined organic layers were dried (Na$_2$SO$_4$) and concentrated under reduced pressure. Flash chromatography (SiO$_2$, 5−10% EtOAc/hexanes, gradient elution) provided **33** (195 mg, 77% yield) as a colorless liquid: ^{1}H NMR (400 MHz, CDCl$_3$) δ ppm 7.32−7.43 (2 H, m), 7.26 (2 H, d, J = 2.3 Hz), 7.12−7.22 (3 H, m), 6.93−7.09 (1 H, m), 4.61 (1 H, d, J = 8.2 Hz), 3.59 (3 H, s), 2.91 (1 H, q, J = 8.2 Hz), 1.96−2.23 (2 H, m), 1.82 (2 H, q, J = 7.6 Hz).

(±)-(5S,6S)-5-(3-Chlorophenyl)-6-(4-chlorophenyl)piperidin-2-one (34). To a solution of **33** (195 mg, 0.516 mmol) in THF/H$_2$O (4:1, 5 mL) was added trimethylphosphine (1.0 M solution in THF, 0.65 mL, 0.65 mmol). After the mixture was stirred for 1 h at 25 °C, the residue was basified (ice-cold 2 M LiOH) and extracted (2 × EtOAc). The combined organic layers were washed (2 × brine), dried (Na$_2$SO$_4$), and concentrated under reduced pressure to provide the crude (±)-(4S,5S)-methyl 5-amino-4-(3-chlorophenyl)-5-(4-chlorophenyl)pentanoate as a colorless film.

The crude amine was dissolved in MeOH/saturated aqueous NaHCO$_3$(4:1, 35 mL), and the mixture was refluxed for 3 h. After MeOH was removed under reduced pressure, the residue was diluted (water) and extracted (3 × DCM). The combined organic layers were washed (1 × brine), dried (Na$_2$SO$_4$), and concentrated under reduced pressure. Flash chromatography (SiO$_2$, 80−100% EtOAc/hexanes, gradient elution) provided **34** (115 mg, 70% yield) as a whilte soild: ^{1}H NMR (400 MHz, CDCl$_3$) δ ppm 7.18−7.23 (1 H, m), 7.10−7.17 (3 H, m), 6.84 (1 H, t, J = 1.8 Hz), 6.62−6.69 (3 H, m), 6.18 (1 H, br s), 4.77 (1 H, t, J = 4.5 Hz), 3.47−3.55 (1 H, m), 2.73−2.83 (1 H, m), 2.58−2.71 (1 H, m), 2.08−2.21 (1 H, m), 1.81−1.90 (1 H, m); MS (ESI) 319.9 [M + H][+].

(±)-(5S,6S)-5-(3-Chlorophenyl)-6-(4-chlorophenyl)-1-(cyclopropylmethyl)piperidin-2-one (35). To a solution of **34** (300 mg, 0.937 mmol) in DMF (3.8 mL) was added NaH (60% in mineral oil, 49 mg, 1.22 mmol) at 0 °C. The mixture was stirred at 0 °C for 20 min and then treated with cyclopropylmethyl bromide (152 μL, 1.12 mmol). After the mixture was stirred at 25 °C for 5 h, the reaction was quenched (saturated aqueous NH$_4$Cl), extracted (2 × EtOAc), and washed (brine). The combined organic layers were dried (Na$_2$SO$_4$) and concentrated under reduced pressure. Flash chromatography (SiO$_2$, 30−50% EtOAc/hexanes, gradient elution) provided **35** (294 mg, 84% yield) as a colorless foam: ^{1}H NMR (400 MHz, CDCl$_3$) δ ppm 7.19−7.24 (1 H, m), 7.11−7.17 (3 H, m), 6.86 (1 H, t, J = 1.8 Hz), 6.65 (1 H, d, J = 7.4 Hz), 6.55 (2 H, d, J = 8.6 Hz), 4.85 (1 H, d, J = 4.7 Hz), 3.91 (1 H, dd, J = 14.1, 6.3 Hz), 3.53 (1 H, ddd, J = 13.4, 5.0, 2.7 Hz), 2.82−2.90 (1 H, m), 2.67−2.78 (1 H, m), 2.44 (1 H, dd, J = 14.1, 7.8 Hz), 2.04−2.20 (1 H, m), 1.78−1.85 (1 H, m), 0.88−0.98 (1 H, m), 0.52 (1 H, tt, J = 8.7, 4.6 Hz), 0.36−0.44 (1 H, m), 0.05−0.20 (2 H, m); MS (ESI) 373.9 [M + H][+].

(±)-(3R,5S,6S)-3-Allyl-5-(3-chlorophenyl)-6-(4-chlorophenyl)-1-(cyclopropylmethyl)piperidin-2-one (36). To a solution of **35** (275 mg, 0.735 mmol) and allyl bromide (67 μL, 0.77 mmol) in THF (3.6 mL) was added LiHMDS (1 M in THF, 0.81 mL, 0.81 mmol) at −78 °C dropwise. After the mixture was stirred at −78 °C for 3 h, the reaction was quenched (saturated aqueous NH$_4$Cl), extracted (2 × EtOAc), and washed (brine). The combined organic layers were dried (Na$_2$SO$_4$) and concentrated under reduced pressure. Flash chromatography (SiO$_2$, 20−30% EtOAc/hexanes, gradient elution) provided **36** (256 mg, 84% yield) as a colorless oil: ^{1}H NMR (400 MHz, CDCl$_3$) δ ppm 7.17−7.24 (1 H, m), 7.14 (3 H, t, J = 8.0 Hz), 6.88 (1 H, s), 6.65 (1 H, d, J = 7.4 Hz), 6.54 (2 H, d, J = 8.6 Hz), 5.73−6.02 (1 H, m), 5.05−5.12 (2 H, m), 4.81 (1 H, d, J = 4.7 Hz), 3.92 (1 H, dd, J = 14.1, 6.3 Hz), 3.56−3.64 (1 H, m), 2.77−2.87 (2 H, m), 2.40−2.53 (2 H, m), 2.11−2.22 (1 H, m), 1.71−1.78 (1 H, m), 0.85−1.00 (1 H, m), 0.47−0.58 (1 H, m), 0.36−0.43 (1 H, m), 0.13−0.21 (1 H, m), 0.02−0.11 (1 H, m); MS (ESI) 414.0 [M + H][+].

(±)-2-((3S,5S,6S)-5-(3-Chlorophenyl)-6-(4-chlorophenyl)-1-(cyclopropylmethyl)-2-oxopiperidin-3-yl)acetic Acid (1). To a rapidly stirring solution of **36** (27 mg, 0.064 mmol) and RuCl$_3$ hydrate (1.4 mg, 0.0064 mmol) in H$_2$O/CCl$_4$/AcCN (1.5:1:1, 1.3 mL) was added NaIO$_4$ (55 mg, 0.26 mmol) in 4 portions over 20 min while maintaining the temperature below 25 °C. After being stirred vigorously for 3 h, the mixture was filtered through Celite and the filter cake was washed (EtOAc). The filtrate was extracted (2 × EtOAc) and washed (2 × 10% aqueous NaHSO$_3$ and 1 × brine). The combined organic layers were dried (Na$_2$SO$_4$) and concentrated under reduced pressure. Purification by RP-HPLC (10−90% A/B, gradient elution) provided **1** (22 mg, 79% yield) as a white solid: ^{1}H NMR (400 MHz, CDCl$_3$) δ ppm 7.23−7.26 (1 H, m), 7.13−7.19 (3 H, m), 6.87 (1 H, t, J = 1.6 Hz), 6.63 (1 H, d, J = 7.8 Hz), 6.54 (2 H, d, J = 8.6

Hz), 4.87 (1 H, d, J = 5.1 Hz), 3.85 (1 H, dd, J = 14.1, 6.7 Hz), 3.51–3.58 (1 H, m), 3.33–3.41 (1 H, m), 3.14 (1 H, dd, J = 16.4, 7.0 Hz), 2.72 (1 H, dd, J = 16.6, 6.5 Hz), 2.59 (1 H, dd, J = 14.1, 7.4 Hz), 2.36–2.50 (1 H, m), 1.70 (1 H, d, J = 13.7 Hz), 0.87–1.01 (1 H, m), 0.51–0.61 (1 H, m), 0.40–0.50 (1 H, dd, J = 8.2, 4.7 Hz), 0.14–0.24 (1 H, m), 0.03–0.13 (1 H, m); MS (ESI) 431.9 [M + H]$^+$, 429.9 [M − H]$^-$.

(±)-(4S,5R)-Methyl 5-Azido-4-(3-chlorophenyl)-5-(4-chlorophenyl)pentanoate (37). To a solution of **32** (5.14 g, 14.5 mmol) and TEA (4.06 mL, 29.1 mmol) in DCM (72 mL) was added MsCl (1.47 mL, 18.9 mmol) dropwise at 0 °C, and the resulting solution was stirred at 0 °C for 1 h. The reaction was quenched (ice-cold water), extracted (3 × DCM), and washed (brine). The combined organic layers were dried (Na$_2$SO$_4$) and concentrated under reduced pressure to provide a crude mesylated intermediate.

The residue above was dissolved in DMF (40 mL), and NaN$_3$ (4.73 g, 72.8 mmol) was added. After being stirred at 90 °C for 30 min, the mixture was cooled to 25 °C, diluted (water), extracted (2 × EtOAc), and washed (3 × brine). The combined organic layers were dried (Na$_2$SO$_4$) and concentrated under reduced pressure. Flash column chromatography (SiO$_2$, 5−7% EtOAc/hexanes, gradient elution) provided **37** (3.10 g, 56% yield) as a colorless liquid: ^{1}H NMR (400 MHz, CDCl$_3$) δ ppm 7.19−7.26 (2 H, m), 7.10−7.18 (2 H, m), 7.02−7.05 (2 H, m), 6.97−7.01 (1 H, m), 6.81−6.86 (1 H, m), 4.58 (1 H, d, J = 8.2 Hz), 3.62 (3 H, s), 2.84−2.93 (1 H, m), 2.35−2.45 (1 H, m), 2.06−2.18 (2 H, m), 1.87−2.02 (1 H, m).

(±)-(5R,6S)-5-(3-Chlorophenyl)-6-(4-chlorophenyl)piperidin-2-one (3). To a solution of **37** (3.10 g, 8.20 mmol) in THF/H$_2$O (4:1, 40 mL) was added Me$_3$P (1.0 M in THF, 10.2 mL, 10.2 mmol). After the mixture was stirred for 1 h at 25 °C, the residues were basified (ice-cold 2 M aqueous LiOH) and the product was extracted (3 × EtOAc) and washed (2 × brine). The combined organic layers were dried (Na$_2$SO$_4$) and concentrated under reduced pressure to provide the crude amine as a colorless film.

The crude amine above was dissolved in MeOH/saturated aqueous NaHCO$_3$ (4:1, 380 mL), and the mixture was refluxed overnight. After most of the MeOH was removed under reduced pressure, the residue was diluted (water) and extracted (3 × EtOAc). The combined organic layers were washed (1 × brine), dried (Na$_2$SO$_4$), and concentrated under reduced pressure. Flash column chromatography (SiO$_2$, 80−100% EtOAc/hexanes, gradient elution) provided **3** (2.30 g, 88% yield) as a white solid: ^{1}H NMR (400 MHz, CDCl$_3$) δ ppm 7.20−7.24 (2 H, m), 7.11−7.20 (2 H, m), 7.01−7.04 (1 H, m), 6.95−6.98 (2 H, m), 6.76−6.80 (1 H, m), 5.83 (1 H, s, br), 4.51 (1 H, d, J = 9.8 Hz), 2.78−2.88 (1 H, m), 2.62−2.68 (2 H, m), 2.20−2.32 (1 H, m), 2.07−2.19 (1 H, m); HRMS (ESI) m/z 320.0586 [M + H]$^+$ (C$_{17}$H$_{15}$Cl$_2$NO requires 320.0601).

(5R,6S)-5-(3-Chlorophenyl)-6-(4-chlorophenyl)piperidin-2-one [(5R,6S)-3] and (5S,6R)-5-(3-Chlorophenyl)-6-(4-chlorophenyl)piperidin-2-one [(5S,6R)-3]. Individual stereoisomers in **3** were separated by chiral HPLC [flow rate, 18 mL/min on a Chiralcel OD-H 20 mm i.d. × 250 mm, 5 μm column (Daicel Inc., Fort Lee, NJ), using 40% isopropyl alcohol/hexanes as the eluent] to give (5R,6S)-**3** (t_R = 8.2 min) and (5S,6R)-**3** (t_R = 12.4 min) as a white solid. (5S,6R)-**3**: $[\alpha]^{23}_D$ +158° (c 1.12, MeOH). (5R,6S)-**3**: $[\alpha]^{23}_D$ −156° (c 1.13, MeOH).

(±)-(5R,6S)-5-(3-Chlorophenyl)-6-(4-chlorophenyl)-1-(cyclopropylmethyl)piperidin-2-one (4). Compound **4** was prepared as a colorless foam from **3** according to a similar procedure described for the synthesis of **35**: ^{1}H NMR (500 MHz, CDCl$_3$) δ ppm 7.28−7.32 (2 H, m), 7.19−7.25 (3 H, m), 6.97−7.02 (3 H, m), 4.84 (1 H, d, J = 6.1 Hz), 4.06−4.12 (1 H, m), 2.97−3.04 (1 H, m), 2.45−2.60 (2 H, m), 2.23−2.29 (1 H, m), 2.06−2.14 (1 H, m), 1.95−2.04 (1 H, m), 0.96−1.05 (1 H, m), 0.52−0.60 (1 H, m), 0.42−0.50 (1 H, m), 0.08−0.22 (2 H, m); HRMS (ESI) m/z 374.1060 [M + H]$^+$ (C$_{21}$H$_{21}$Cl$_2$NO requires 374.1069).

Compounds (5R,6S)-**4** and (5S,6R)-**4** were prepared from (5R,6S)-**3** and (5S,6R)-**3**, respectively, according to a similar procedure described for the synthesis of **35**.

Compounds **5−8** and **13** were prepared from **3** according to a similar procedure described for the synthesis of **35**.

(±)-(5R,6S)-5-(3-Chlorophenyl)-6-(4-chlorophenyl)-1-propylpiperidin-2-one (5). ^{1}H NMR (400 MHz, CDCl$_3$) δ ppm 7.26−7.30 (2 H, m), 7.14−7.24 (2 H, m), 7.06−7.08 (1 H, m), 6.93−6.97 (2 H, m), 6.84−6.88 (1 H, m), 4.53 (1 H, d, J = 7.8 Hz), 3.84−3.93 (1 H, m), 2.93−3.00 (1 H, m), 2.56−2.69 (2 H, m), 2.40−2.50 (1 H, m), 2.01−2.09 (2 H, m), 1.48−1.60 (2 H, m), 0.83 (3 H, t, J = 7.2 Hz); HRMS (ESI) m/z 362.1060 [M + H]$^+$ (C$_{20}$H$_{21}$Cl$_2$NO requires 362.1069).

(±)-(5R,6S)-5-(3-Chlorophenyl)-6-(4-chlorophenyl)-1-isobutylpiperidin-2-one (6). ^{1}H NMR (400 MHz, CDCl$_3$) δ ppm 7.25−7.27 (2 H, m), 7.15−7.24 (2 H, m), 7.03−7.06 (1 H, m), 6.86−6.93 (2 H, m), 6.80−6.83 (1 H, m), 4.49 (1 H, d, J = 8.6 Hz), 3.87−3.96 (1 H, m), 2.88−2.96 (1 H, m), 2.74−2.82 (1 H, m), 2.60−2.72 (1 H, m), 1.88−2.22 (4 H, m), 0.87 (3 H, d, J = 6.6 Hz), 0.83 (3 H, d, J = 6.3 Hz); HRMS (ESI) m/z 376.1243 [M + H]$^+$ (C$_{21}$H$_{23}$Cl$_2$NO requires 376.1225).

(±)-(5R,6S)-1-Butyl-5-(3-chlorophenyl)-6-(4-chlorophenyl)piperidin-2-one (7). ^{1}H NMR (400 MHz, CDCl$_3$) δ ppm 7.27−7.30 (2 H, m), 7.15−7.24 (2 H, m), 7.06−7.08 (1 H, m), 6.93−6.97 (2 H, m), 6.83−6.87 (1 H, m), 4.53 (1 H, d, J = 7.8 Hz), 3.88−3.96 (1 H, m), 2.93−3.00 (1 H, m), 2.55−2.79 (2 H, m), 2.42−2.51 (1 H, m), 2.02−2.10 (2 H, m), 1.44−1.52 (2 H, m), 1.15−1.30 (2 H, m), 0.86 (3 H, t, J = 7.4 Hz); HRMS (ESI) m/z 376.1216 [M + H]$^+$ (C$_{21}$H$_{23}$Cl$_2$NO requires 376.1225).

(±)-(5R,6S)-1-Benzyl-5-(3-chlorophenyl)-6-(4-chlorophenyl)piperidin-2-one (8). ^{1}H NMR (400 MHz, CDCl3) δ ppm 7.28−7.32 (3 H, m), 7.22−7.25 (2 H, m), 7.05−7.17 (3 H, m), 6.98−7.05 (1 H, m), 6.86−6.92 (2 H, m), 6.78−6.82 (1 H, m), 6.57−6.61 (1 H, m), 5.55 (1 H, d, J = 14.5 Hz), 4.38 (1 H, d, J = 7.0 Hz), 3.35 (1 H, d, J = 14.5 Hz), 2.91−2.97 (1 H, m), 2.63−2.70 (2 H, m), 1.92−2.10 (2 H, m); HRMS (ESI) m/z 410.1068 [M + H]$^+$ (C$_{24}$H$_{21}$Cl$_2$NO requires 410.1069).

(±)-Methyl 2-((2S,3R)-3-(3-Chlorophenyl)-2-(4-chlorophenyl)-6-oxopiperidin-1-yl)acetate (13). ^{1}H NMR (400 MHz, CDCl$_3$) δ ppm 7.22−7.26 (2 H, m), 7.13−7.21 (2 H, m), 7.08−7.11 (1 H, m), 6.86−6.94 (3 H, m), 4.63 (1 H, d, J = 9.0 Hz), 4.58 (1 H, d, J = 17.2 Hz), 3.71 (3 H, s), 3.18 (1 H, d, J = 17.2 Hz), 2.93−3.01 (1 H, m), 2.60−2.76 (2 H, m), 2.20−2.32 (1 H, m), 2.06−2.13 (1 H, m); HRMS (ESI) m/z 392.0847 [M + H]$^+$ (C$_{20}$H$_{19}$Cl$_2$NO$_3$ requires 392.0811).

(±)-(S)-Ethyl 2-((2S,3R)-3-(3-Chlorophenyl)-2-(4-chlorophenyl)-6-oxopiperidin-1-yl)butanoate (9) and (±)-(R)-Ethyl 2-((2S,3R)-3-(3-Chlorophenyl)-2-(4-chlorophenyl)-6-oxopiperidin-1-yl)butanoate (10). To a solution of **3** (442 mg, 1.38 mmol) in DMF (4.0 mL) was added NaH (60% in mineral oil, 221 mg, 5.52 mmol) at 0 °C. After the mixture was stirred for 20 min at 0 °C, ethyl 2-bromobutyrate (1.02 mL, 6.90 mmol) was added at 0 °C. Then the mixture was allowed to warm to 25 °C and stirred for 24 h. The reaction was quenched (saturated aqueous NH$_4$Cl), extracted (2 × EtOAc), and washed (3 × H$_2$O and 1 × brine). The combined organic layers were dried (Na$_2$SO$_4$) and concentrated under reduced pressure. Flash column chromatography (SiO$_2$, 20%, 30%, and 40% EtOAc/hexanes) provided **9** (320 mg, 53%) as a colorless foam and **10** (181 mg, 30%) as a white solid successively. Compound **9**: ^{1}H NMR (400 MHz, CDCl$_3$) δ ppm 7.25 (2 H, d, J = 8.2 Hz), 7.10−7.22 (2 H, m), 7.04−7.06 (1 H, m), 7.01 (2 H, d, J = 8.2 Hz), 6.83 (1 H, d, J = 7.0 Hz), 4.56 (1 H, d, J = 9.0 Hz), 4.05−4.16 (2 H, m), 3.36−3.42 (1 H, m), 3.00−3.08 (1 H, m), 2.63−2.68 (2 H, m), 2.15−2.31 (2 H, m), 2.05−2.12 (1 H, m), 1.54−1.65 (1 H, m), 1.28 (3 H, t, J = 7.2 Hz), 0.62 (3 H, t, J = 7.4 Hz); HRMS (ESI) m/z 434.1265 [M + H]$^+$ (C$_{23}$H$_{25}$Cl$_2$NO$_3$ requires 434.1279). Compound **10**: ^{1}H NMR (400 MHz, CDCl$_3$) δ ppm 7.23 (2 H, d, J = 8.6 Hz), 7.11−7.20 (2 H, m), 7.09 (2 H, d, J = 8.6 Hz), 6.99−7.03 (1 H, m), 6.76−6.80 (1 H, m), 4.50 (1 H, d, J = 9.4 Hz), 4.06−4.20 (2 H, m), 3.33 (1 H, t, J = 7.0 Hz), 2.96−3.04 (1 H, m), 2.63−2.73 (2 H, m), 2.05−2.19 (3 H, m), 1.88−1.98 (1 H, m), 1.26 (3 H, t, J = 7.0 Hz), 1.00 (3 H, t, J = 7.4 Hz); HRMS (ESI) m/z 434.1285 [M + H]$^+$ (C$_{23}$H$_{25}$Cl$_2$NO$_3$ requires 434.1279).

Compounds **11** and **12** were prepared according to a similar procedure described for the synthesis of **9**.

(±)-(S)-Ethyl 2-((2S,3R)-3-(3-Chlorophenyl)-2-(4-chlorophenyl)-6-oxopiperidin-1-yl)pentanoate (11). ^{1}H NMR (400 MHz, CDCl$_3$) δ ppm 7.25 (2 H, d, J = 8.6 Hz), 7.11−7.20 (2 H, m), 7.04−7.06 (1 H, m), 7.02 (2 H, d, J = 8.6 Hz), 6.82−6.85 (1 H, m), 4.57 (1 H, d, J = 9.4 Hz), 4.08−4.15 (2 H, m), 3.45−3.49 (1 H, m), 2.99−3.06 (1 H, m), 2.63−2.68 (2 H, m), 2.13−2.28 (2 H, m), 2.04−2.12 (1 H, m), 1.43−1.52 (1 H, m), 1.28 (3 H, t, J = 7.0 Hz), 1.05−1.17 (1 H, m), 0.80−0.92 (1 H, m), 0.62 (3 H, t, J = 7.4 Hz); HRMS (ESI) m/z 448.1428 [M + H]$^+$ (C$_{24}$H$_{27}$Cl$_2$NO$_3$ requires 448.1435).

(±)-(S)-Ethyl 2-((2S,3R)-3-(3-Chlorophenyl)-2-(4-chlorophenyl)-6-oxopiperidin-1-yl)propaneate (12). ^{1}H NMR (400 MHz, CDCl$_3$) δ ppm 7.26 (2 H, d, J = 8.6 Hz), 7.11−7.21 (2 H, m), 7.04−7.07 (1 H, m), 7.01 (2 H, d, J = 8.6 Hz), 6.81−6.86 (1 H, m), 4.57 (1 H, d, J = 9.0 Hz), 4.15−4.26 (2 H, m), 3.40 (1 H, q, J = 6.8 Hz), 2.93−3.02 (1 H, m), 2.60−2.66 (2 H, m), 2.14−2.26 (1 H, m), 2.05−2.14 (1 H, m), 1.34 (3 H, d, J = 7.0 Hz), 1.30 (3 H, t, J = 7.4 Hz); HRMS (ESI) m/z 420.1113 [M + H]$^+$ (C$_{22}$H$_{23}$Cl$_2$NO$_3$ requires 420.1123).

(3S,5R,6S)-3-Allyl-5-(3-chlorophenyl)-6-(4-chlorophenyl)-1-(cyclopropylmethyl)piperidin-2-one (15) and (3R,5R,6S)-3-Allyl-5-(3-chlorophenyl)-6-(4-chlorophenyl)-1-(cyclopropylmethyl)piperidin-2-one (38). To a solution of (5R,6S)-4 (433 mg, 1.16 mmol) and allyl bromide (105 μL, 1.22 mmol) in THF (4.6 mL) was added LiHMDS (1 M in THF, 1.27 mL, 1.27 mmol) dropwise at −78 °C. After the mixture was stirred at −78 °C for 3 h, the reaction was quenched (saturated aqueous NH$_4$Cl), extracted (2 × EtOAc), and washed (brine). The combined organic layers were dried (Na$_2$SO$_4$) and concentrated under reduced pressure. Flash column chromatography (SiO$_2$, 15−20% MTBE/hexanes, gradient elution) provided less polar minor diastereomer 15 (105 mg, 25% yield) and more polar major diastereomer 38 (246 mg, 60% yield) as colorless oils. Compound 15: ^{1}H NMR (400 MHz, CDCl$_3$) δ ppm 7.41−7.43 (1 H, m), 7.34 (2 H, d, J = 8.2 Hz), 7.24−7.27 (2 H, m), 7.16−7.21 (1 H, m), 7.05 (2 H, d, J = 8.2 Hz), 5.70−5.83 (1 H, m), 5.00−5.09 (3 H, m), 4.11−4.18 (1 H, m), 3.11−3.15 (1 H, m), 2.62−2.70 (1 H, m), 2.42−2.50 (1 H, m), 2.32−2.38 (1 H, m), 2.24−2.30 (1 H, m), 1.95−2.02 (1 H, m), 1.83−1.90 (1 H, m), 1.08−1.16 (1 H, m), 0.50−0.65 (2 H, m), 0.18−0.27 (2 H, m); HRMS (ESI) m/z 414.1386 [M + H]$^+$ (C$_{24}$H$_{25}$Cl$_2$NO requires 414.1381). Compound 38: ^{1}H NMR (400 MHz, CDCl$_3$) δ ppm 7.21 (2 H, t, J = 8.2 Hz), 7.17−7.19 (1 H, m), 7.11−7.15 (1 H, m), 7.02−7.04 (1 H, m), 6.85 (2 H, d, J = 8.2 Hz), 6.72−6.77 (1 H, m), 5.77−5.88 (1 H, m), 5.05−5.15 (2 H, m), 4.60 (1 H, d, J = 10.2 Hz), 3.93−3.98 (1 H, m), 2.88−2.96 (1 H, m), 2.78−2.85 (1 H, m), 2.59−2.68 (1 H, m), 2.37−2.45 (1 H, m), 2.22−2.30 (1 H, m), 1.96−2.09 (2 H, m), 0.83−0.92 (1 H, m), 0.45−0.53 (1 H, m), 0.36−0.44 (1 H, m), 0.09−0.15 (1 H, m), −0.02 to 0.04 (1 H, m); MS (ESI) 414.2 [M + H]$^+$.

2-((3R,5R,6S)-5-(3-Chlorophenyl)-6-(4-chlorophenyl)-1-(cyclopropylmethyl)-2-oxopiperidin-3-yl)acetic Acid (2). To a rapidly stirring solution of 15 (1.20 g, 2.90 mmol) and RuCl$_3$ hydrate (65.3 mg, 0.290 mmol) in H$_2$O/CCl$_4$/AcCN (1.5:1:1, 30 mL) was added NaIO$_4$ (2.48 g, 11.6 mmol) in four portions over 40 min while maintaining the temperature below 25 °C. After being stirred vigorously for 16 h, the mixture was filtered through Celite and the filter cake was washed (EtOAc). The filtrate was extracted (2 × EtOAc) and washed (2 × 10% aqueous NaHSO$_3$ and 1 × brine). The combined organic layers were dried (Na$_2$SO$_4$) and concentrated under reduced pressure. Purification by RP-HPLC (10−90% A/B, gradient elution) provided 2 (1.03 g, 78% yield) as a white solid: ^{1}H NMR (400 MHz, CDCl$_3$) δ ppm 7.46−7.49 (1 H, s), 7.40 (2 H, d, J = 8.6 Hz), 7.32−7.35 (2 H, m), 7.22−7.26 (1 H, m), 7.13 (2 H, d, J = 8.6 Hz), 5.17 (1 H, s, br), 4.21−4.27 (1 H, m), 3.18−3.23 (1 H, m), 2.80−2.87 (1 H, m), 2.53−2.62 (1 H, m), 2.46−2.53 (1 H, m), 2.32−2.40 (1 H, m), 2.05−2.15 (1 H, m), 1.83−1.92 (1 H, m), 1.15−1.26 (1 H, m), 0.68−0.76 (1 H, m), 0.58−0.66 (1 H, m), 0.25−0.36 (2 H, m); HRMS (ESI) m/z 432.1133 [M + H]$^+$ (C$_{23}$H$_{23}$Cl$_2$NO$_3$ requires 432.1128).

2-((3S,5R,6S)-5-(3-Chlorophenyl)-6-(4-chlorophenyl)-1-(cyclopropylmethyl)-2-oxopiperidin-3-yl)acetic Acid (14). Compound 14 was prepared as a white solid from 38 according to a similar procedure described for the synthesis of 2: ^{1}H NMR (400 MHz, CDCl$_3$) δ ppm 7.24 (2 H, d, J = 8.2 Hz), 7.18−7.22 (1 H, m), 7.12−

7.16 (1 H, m), 6.98−7.02 (1 H, m), 6.86 (2 H, d, J = 8.2 Hz), 6.72−6.75 (1 H, m), 4.63 (1 H, d, J = 10.2 Hz), 3.89−3.96 (1 H, m), 2.93−3.10 (3 H, m), 2.56−2.63 (1 H, m), 2.31−2.38 (1 H, m), 2.08−2.25 (2 H, m), 0.85−0.95 (1 H, m), 0.48−0.55 (1 H, m), 0.40−0.46 (1H, m), 0.08−0.16 (1H, m), −0.02 to 0.06 (1 H, m); HRMS (ESI) m/z 432.1140 [M + H]$^+$ (C$_{23}$H$_{23}$Cl$_2$NO$_3$ requires 432.1128).

(3S,5R,6S)-3-(But-3-en-1-yl)-5-(3-chlorophenyl)-6-(4-chlorophenyl)-1-(cyclopropylmethyl)piperidin-2-one (39) and (3R,5R,6S)-3-(But-3-en-1-yl)-5-(3-chlorophenyl)-6-(4-chlorophenyl)-1-(cyclopropylmethyl)piperidin-2-one (40). To a solution of (5R,6S)-4 (630 mg, 1.68 mmol) and 4-bromo-1-butene (1.11 mL, 10.9 mmol) in THF (12 mL) was added LiHMDS (1.0 M in THF, 10.1 mL, 10.1 mmol) at 0 °C, and the resulting solution was heated to 40 °C and stirred for 3 h. The reaction was quenched (saturated aqueous NH$_4$Cl) and extracted (3 × EtOAc). The combined organic layers were washed (brine), dried (Na$_2$SO$_4$), and concentrated under reduced pressure. Flash column chromatography (SiO$_2$, 4−30% EtOAc/hexanes, gradient elution) provided a mixture of two diastereomers (304 mg, 42% yield, dr = 1.5/1 in favor of 39).

Individual stereoisomers in a mixture above were separated by chiral HPLC [flow rate, 18 mL/min on a Chiralcel OD-H 20 mm i.d. × 250 mm, 5 mic column (Daicel Inc., Fort Lee, NJ), using 2% isopropyl alcohol/hexanes as the eluent] to give 40 and 39 successively. Compound 39: ^{1}H NMR (400 MHz, CDCl$_3$) δ ppm 7.37−7.40 (1 H, m), 7.33 (2 H, d, J = 8.4 Hz), 7.23−7.26 (2 H, m), 7.12−7.19 (1 H, m), 7.03 (2 H, d, J = 8.4 Hz), 5.72−5.84 (1 H, m), 4.93−5.04 (3 H, m), 4.13 (1 H, dd, J = 14.1, 6.5 Hz), 3.11−3.16 (1 H, m), 1.88−2.36 (7 H, m), 1.62−1.70 (1 H, m), 1.03−1.14 (1 H, m), 0.46−0.65 (2 H, m), 0.13−0.25 (2 H, m); MS (ESI) 428.2 [M + H]$^+$. Compound 40: ^{1}H NMR (400 MHz, CDCl$_3$) δ ppm 7.11−7.25 (4 H, m), 6.98−7.03 (1 H, m), 6.80−6.83 (2 H, m), 6.72−6.77 (1 H, m), 5.77−5.89 (1 H, m), 4.95−5.10 (2 H, m), 4.59 (1 H, d, J = 10.2 Hz), 3.95 (1 H, dd, J = 14.2, 6.6 Hz), 2.85−2.95 (1 H, m), 2.50−2.60 (1 H, m), 1.97−2.30 (6 H, m), 1.62−1.71 (1 H, m), 0.82−0.92 (1 H, m), 0.34−0.53 (2 H, m), −0.05 to 0.17 (2 H, m); MS (ESI) 428.2 [M + H]$^+$.

3-((3S,5R,6S)-5-(3-Chlorophenyl)-6-(4-chlorophenyl)-1-(cyclopropylmethyl)-2-oxopiperidin-3-yl)propanoic Acid (16). Compound 16 was prepared as a white solid from 39 according to a similar procedure described for the synthesis of 2: ^{1}H NMR (400 MHz, CDCl$_3$) δ ppm 7.33 (2 H, d, J = 8.4 Hz), 7.20−7.27 (3 H, m), 7.01−7.06 (1 H, m), 6.98 (2 H, d, J = 8.4 Hz), 4.90 (1 H, d, J = 5.1 Hz), 4.07 (1 H, dd, J = 14.1, 6.5 Hz), 3.09−3.18 (1 H, m), 2.53−2.63 (3 H, m), 2.27−2.35 (1 H, m), 2.17−2.27 (1 H, m), 2.06−2.15 (1 H, m), 1.87 − 2.03 (2 H, m), 1.00−1.10 (1 H, m), 0.56−0.65 (1 H, m), 0.46−0.54 (1 H, m), 0.10−0.25 (2 H, m); HRMS (ESI) m/z 446.1283 [M + H]$^+$ (C$_{24}$H$_{25}$Cl$_2$NO$_3$ requires 446.1291).

3-((3R,5R,6S)-5-(3-Chlorophenyl)-6-(4-chlorophenyl)-1-(cyclopropylmethyl)-2-oxopiperidin-3-yl)propanoic Acid (17). Compound 17 was prepared as a white solid from 40 according to a similar procedure described for the synthesis of 2: ^{1}H NMR (400 MHz, CDCl$_3$) δ ppm 7.22 (2 H, d, J = 8.2 Hz), 7.11−7.20 (2 H, m), 7.01 (1 H, s), 6.85 (2 H, d, J = 8.4 Hz), 6.75 (1 H, d, J = 7.4 Hz), 4.61 (1 H, d, J = 10.0 Hz), 3.92 (1 H, dd, J = 14.3, 6.5 Hz), 2.90−3.01 (1 H, m), 2.47−2.78 (3 H, m), 2.21−2.36 (2 H, m), 1.90−2.15 (3 H, m), 0.81−0.93 (1 H, m), 0.45−0.54 (1 H, m), 0.37−0.45 (1 H, m), 0.07−0.15 (1 H, m), −0.04 to 0.04 (1 H, m); HRMS (ESI) m/z 446.1283 [M + H]$^+$ (C$_{24}$H$_{25}$Cl$_2$NO$_3$ requires 446.1291).

Methyl 2-((3R,5R,6S)-5-(3-Chlorophenyl)-6-(4-chlorophenyl)-1-(cyclopropylmethyl)-2-oxopiperidin-3-yl)acetate (18). To a suspension of 2 (250 mg, 578 μmol) in MeOH (3 mL) was added thionyl chloride (78 μL, 1.1 mmol) dropwise at 0 °C. After being stirred at 25 °C overnight, the mixture was diluted (EtOAc), basified (saturated aqueous NaHCO$_3$), extracted (2 × EtOAc), and washed (brine). The combined organic layers were dried (Na$_2$SO$_4$) and concentrated under reduced pressure to provide 18 (230 mg, 89% yield) as a colorless liquid: ^{1}H NMR (400 MHz, CDCl$_3$) δ ppm 7.48−7.52 (1 H, m), 7.39 (2 H, d, J = 8.6 Hz), 7.28−7.31 (2 H, m), 7.25−7.27 (1 H, m), 7.24 (2 H, d, J = 8.6 Hz), 5.12 (1 H, s, br), 4.18−4.26 (1 H, m), 3.69 (3 H, s), 3.16−3.20 (1 H, m), 2.78−2.85 (1 H, m), 2.62−2.68 (1 H, m), 2.53−2.61 (1 H, m), 2.20−2.32 (2 H, m), 1.78−

1.85 (1 H, m), 1.12–1.22 (1 H, m), 0.62–0.70 (1 H, m), 0.52–0.59 (1 H, m), 0.20–0.30 (2 H, m); HRMS (ESI) *m/z* 446.1285 [M + H]⁺ (C₂₄H₂₅Cl₂NO₃ requires 446.1279).

2-((3R,5R,6S)-5-(3-Chlorophenyl)-6-(4-chlorophenyl)-1-(cyclopropylmethyl)-2-oxopiperidin-3-yl)acetamide (19). In a tube, **18** (60 mg, 130 μmol) was treated with ammonia (7 N in MeOH, 4.8 mL, 34 mmol). The tube was sealed and stirred at 25 °C for 5 days. Then NaCN (3 mg) was added, and the resulting solution was stirred at 50 °C for additional 3 days. The mixture was cooled, and excess NH₃ and MeOH were removed under reduced pressure. Purification by RP-HPLC (10–90% A/B, gradient elution) provided **19** (45 mg, 78% yield) as a white solid: ¹H NMR (400 MHz, CDCl₃) δ ppm 7.47–7.52 (1 H, m), 7.37 (2 H, d, *J* = 8.2 Hz), 7.28–7.32 (2 H, m), 7.22–7.26 (1 H, m), 7.17 (2 H, d, *J* = 8.2 Hz), 6.40 (1 H, s, br), 5.42 (1 H, s, br), 5.11 (1 H, s, br), 4.18–4.24 (1 H, m), 3.15–3.20 (1 H, m), 2.69–2.77 (1 H, m), 2.47–2.59 (2 H, m), 2.24–2.34 (2 H, m), 1.85–1.92 (1 H, m), 1.12–1.22 (1 H, m), 0.63–0.72 (1 H, m), 0.54–0.60 (1 H, m), 0.18–0.32 (2 H, m); HRMS (ESI) *m/z* 431.1269 [M + H]⁺ (C₂₃H₂₄Cl₂N₂O₂ requires 431.1283).

2-((3R,5R,6S)-5-(3-Chlorophenyl)-6-(4-chlorophenyl)-1-(cyclopropylmethyl)-2-oxopiperidin-3-yl)acetonitrile (20). A solution of **19** (36 mg, 83 μmol) and TEA (58 μL, 420 μmol) in THF (1.3 mL) was treated with (CF₃CO)₂O (29 μL, 210 μmol) at 0 °C. After the mixture was stirred at 0 °C for 2 h, the reaction was quenched (10% aqueous citric acid), extracted (2 × EtOAc), and washed (brine). The combined organic layers were dried (Na₂SO₄) and concentrated under reduced pressure. Flash column chromatography (SiO₂, 20–30% EtOAc/hexanes, gradient elution) provided **20** (32 mg, 93% yield) as a white foam: ¹H NMR (400 MHz, CDCl₃) δ ppm 7.52–7.55 (1 H, m), 7.41 (2 H, d, *J* = 8.6 Hz), 7.28–7.33 (3 H, m), 7.16 (2 H, d, *J* = 8.6 Hz), 5.18 (1 H, s, br), 4.20–4.25 (1 H, m), 3.25–3.29 (1 H, m), 2.96–3.03 (1 H, m), 2.64–2.71 (1 H, m), 2.44–2.52 (1 H, m), 2.24–2.38 (2 H, m), 1.94–2.01 (1 H, m), 1.15–1.22 (1 H, m), 0.65–0.73 (1 H, m), 0.56–0.63 (1 H, m), 0.23–0.33 (2 H, m); HRMS (ESI) *m/z* 413.1155 [M + H]⁺ (C₂₃H₂₂Cl₂N₂O requires 413.1178).

(3R,5R,6S)-3-((1H-Tetrazol-5-yl)methyl)-5-(3-chlorophenyl)-6-(4-chlorophenyl)-1-(cyclopropylmethyl)piperidin-2-one (21). To a solution of **20** (29 mg, 70 μmol) in DMF (0.18 mL) were added NaN₃ (23 mg, 350 μmol) and NH₄Cl (19 mg, 350 μmol). The mixture was stirred at 90 °C for 2 days. The mixture was cooled to ambient temperature, acidified (10% aqueous citric acid), extracted (2 × EtOAc), and washed (brine). The combined organic layers were dried (Na₂SO₄) and concentrated under reduced pressure. Purification by RP-HPLC (10–90% A/B, gradient elution) provided **21** (13 mg, 41% yield) as a white solid: ¹H NMR (400 MHz, CDCl₃) δ ppm 7.47–7.50 (1 H, m), 7.35 (2 H, d, *J* = 8.6 Hz), 7.29–7.33 (2 H, m), 7.22–7.25 (1 H, m), 6.86 (2 H, d, *J* = 8.6 Hz), 5.14 (1 H, s), 4.19–4.25 (1 H, m), 3.36–3.43 (1 H, m), 3.20–3.24 (1 H, m), 3.11–3.17 (1 H, m), 2.48–2.56 (1 H, m), 2.30–2.37 (1 H, m), 2.15–2.25 (1 H, m), 1.94–2.02 (1 H, m), 1.15–1.23 (1 H, m), 0.69–0.76 (1 H, m), 0.59–0.67 (1 H, m), 0.23–0.36 (2 H, m); HRMS (ESI) *m/z* 456.1361 [M + H]⁺ (C₂₃H₂₃Cl₂N₅O requires 456.1349).

(S)-Ethyl 2-((3S,5R,6S)-3-Allyl-5-(3-chlorophenyl)-6-(4-chlorophenyl)-2-oxopiperidin-1-yl)butanoate (41). (S)-Ethyl 2-((2S,3R)-3-(3-chlorophenyl)-2-(4-chlorophenyl)-6-oxopiperidin-1-yl)butanoate was prepared from (5R,6S)-**3** according to a similar procedure described for the synthesis of **9**.

To a solution of the product above (362 mg, 833 μmol) and allyl bromide (87 μL, 1.00 mmol) in THF (3.3 mL) was added LiHMDS (1 M in THF, 875 μL, 875 μmol) dropwise at −78 °C. After the mixture was stirred at −78 °C for 3 h, the reaction was quenched (saturated aqueous NH₄Cl), extracted (2 × EtOAc), and washed (brine). The combined organic layers were dried (Na₂SO₄) and concentrated under reduced pressure. Flash column chromatography (SiO₂, 15–20% EtOAc/hexanes, gradient elution) provided the C3 epimer of **41** (129 mg, 33% yield) and **41** (183 mg, 46% yield) successively. C3 epimer of **41**: ¹H NMR (400 MHz, CDCl₃) δ ppm 7.23 (2 H, d, *J* = 8.6 Hz), 7.13–7.18 (1 H, m), 7.07–7.13 (1 H, m), 6.97–7.00 (1 H, m), 6.98 (2 H, d, *J* = 8.6 Hz), 6.73–6.77 (1 H, m),

5.76–5.86 (1 H, m), 5.03–5.12 (2 H, m), 4.50 (1 H, d, *J* = 10.6 Hz), 4.12–4.21 (2 H, m), 3.16–3.22 (1 H, m), 3.05–3.14 (1 H, m), 2.74–2.82 (1 H, m), 2.62–2.70 (1 H, m), 2.24–2.38 (2 H, m), 1.96–2.14 (2 H, m), 1.60–1.66 (1 H, m), 1.31 (3 H, t, *J* = 7.2 Hz), 0.60 (3 H, t, *J* = 7.6 Hz); MS (ESI) 474.0 [M + H]⁺. Compound **41**: ¹H NMR (400 MHz, CDCl₃) δ ppm 7.29 (2 H, d, *J* = 8.6 Hz), 7.17–7.21 (2 H, m), 7.13–7.16 (1 H, m), 7.08 (2 H, d, *J* = 8.6 Hz), 6.98–7.02 (1 H, m), 5.77–5.87 (1 H, m), 5.10–5.17 (2 H, m), 4.70 (1 H, d, *J* = 7.4 Hz), 4.07–4.20 (2 H, m), 3.38–3.43 (1 H, m), 3.13–3.20 (1 H, m), 2.68–2.76 (1 H, m), 2.58–2.65 (1 H, m), 2.47–2.57 (1 H, m), 2.21–2.32 (1 H, m), 2.03–2.18 (2 H, m), 1.55–1.62 (1 H, m), 1.28 (3 H, t, *J* = 7.0 Hz), 0.66 (3 H, t, *J* = 7.4 Hz); MS (ESI) 474.0 [M + H]⁺.

(S)-Ethyl 2-((2S,3R,5R)-3-(3-Chlorophenyl)-2-(4-chlorophenyl)-5-(hydroxymethyl)-6-oxopiperidin-1-yl)butanoate (22). 22 was prepared from **41** according to a similar procedure described for the synthesis of **2**: ¹H NMR (400 MHz, CDCl₃) δ ppm 7.34–7.40 (3 H, m), 7.27–7.32 (3 H, m), 7.24–7.26 (2 H, m), 4.91 (1 H, d, *J* = 3.5 Hz), 4.10–4.21 (2 H, m), 3.52–3.56 (1 H, m), 3.16–3.20 (1 H, m), 2.70–2.84 (3 H, m), 2.29–2.38 (2 H, m), 1.95–2.03 (1 H, m), 1.50–1.60 (1 H, m), 1.27 (3 H, t, *J* = 7.4 Hz), 0.70 (3 H, t, *J* = 7.4 Hz); HRMS (ESI) *m/z* 492.1328 [M + H]⁺ (C₂₅H₂₇Cl₂NO₅ requires 492.1333).

(S)-tert-Butyl 2-((3S,5R,6S)-3-Allyl-5-(3-chlorophenyl)-6-(4-chlorophenyl)-2-oxopiperidin-1-yl)butanoate (42). 42 was prepared from (5R,6S)-**3** using *tert*-butyl 2-bromobutyrate according to similar procedures described for the synthesis of **41**: ¹H NMR (400 MHz, CDCl₃) δ ppm 7.25–7.29 (2 H, m), 7.12–7.18 (2 H, m), 7.02–7.09 (3 H, m), 6.88–6.93 (1 H, m), 5.76–5.89 (1 H, m), 5.08–5.17 (2 H, m), 4.64 (1 H, d, *J* = 8.6 Hz), 3.14–3.21 (1 H, m), 3.09–3.14 (1H, m), 2.71–2.78 (1 H, m), 2.62–2.69 (1 H, m), 2.45–2.56 (1 H, m), 2.15–2.30 (2 H, m), 1.98–2.04 (1 H, m), 1.50–1.60 (1 H, m), 1.47 (9 H, s), 0.61 (3 H, t, *J* = 7.6 Hz); MS (ESI) 446.0 [M + H]⁺.

2-((3R,5R,6S)-1-((S)-1-(tert-Butoxy)-1-oxo-butan-2-yl)-5-(3-chlorophenyl)-6-(4-chlorophenyl)-2-oxopiperidin-3-yl)acetic Acid (23). 23 was prepared from **42** according to a similar procedure described for the synthesis of **2**: ¹H NMR (400 MHz, CDCl₃) δ ppm 7.33–7.37 (2 H, m), 7.23–7.29 (3 H, m), 7.16–7.21 (3 H, m), 4.86 (1 H, d, *J* = 4.9 Hz), 3.32–3.37 (1 H, m), 3.13–3.19 (1 H, m), 2.72–2.92 (3 H, m), 2.18–2.34 (2 H, m), 2.05–2.14 (1 H, m), 1.51–1.60 (1 H, m), 1.44 (9 H, s), 0.67 (3 H, t, *J* = 7.4 Hz); HRMS (ESI) *m/z* 520.1635 [M + H]⁺ (C₂₇H₃₁Cl₂NO₅ requires 520.1645).

(S)-tert-Butyl 2-((3R,5R,6S)-3-(2-Amino-2-oxo-ethyl)-5-(3-chlorophenyl)-6-(4-chlorophenyl)-2-oxopiperidin-1-yl)-butanoate (43). To a solution of **23** (195 mg, 0.374 mmol) and N-methylmorpholine (58 μL, 0.53 mmol) in THF (1.8 mL) was added isobutyl chloroformate (59 μL, 0.45 mmol) at 0 °C. The cloudy colorless solution was stirred at 0 °C for 30 min. Then ammonium hydroxide (28% ammonia in water, 51 μL, 0.75 mmol) was added to the mixture at 0 °C, and the resulting mixture was stirred at 0 °C for 1 h. The reaction was quenched (water), extracted (2 × EtOAc), and washed (brine). The combined organic layers were dried (Na₂SO₄) and concentrated under reduced pressure. The residue was purified by RP-HPLC (10–90% A/B, gradient elution) to give **43** (174 mg, 90% yield) as a white solid: ¹H NMR (400 MHz, CDCl₃) δ ppm 7.33 (2 H, d, *J* = 8.4 Hz), 7.19–7.24 (3 H, m), 7.15 (2 H, d, *J* = 8.4 Hz), 7.06–7.12 (1 H, m), 6.72 (1 H, s, br), 4.76 (1 H, d, *J* = 6.3 Hz), 3.17–3.27 (2 H, m), 2.85–2.93 (1 H, m), 2.74–2.83 (2 H, m), 2.24–2.33 (2 H, m), 2.13–2.23 (1 H, m), 1.50–1.57 (1 H, m), 1.47 (9 H, s), 0.64 (3 H, t, *J* = 7.5 Hz); MS (ESI) 519.1 [M + H]⁺

(S)-tert-Butyl 2-((3R,5R,6S)-3-((1H-Tetrazol-5-yl)methyl)-5-(3-chlorophenyl)-6-(4-chlorophenyl)-2-oxopiperidin-1-yl)-butanoate (24). 24 was prepared from **43** according to similar procedures described for the synthesis of **21**: ¹H NMR (400 MHz, CDCl₃) δ ppm 7.32 (2 H, d, *J* = 8.4 Hz), 7.17–7.25 (3 H, m), 7.02–7.06 (1 H, m), 7.00 (2 H, d, *J* = 8.4 Hz), 4.77 (1 H, d, *J* = 6.3 Hz), 3.54–3.61 (1 H, m), 3.36–3.44 (2 H, m), 3.22–3.28 (1 H, m), 2.92–2.98 (1 H, m), 2.16–2.32 (3 H, m), 1.49–1.51 (1 H, m), 1.46 (9 H, s), 0.66 (3 H, t, *J* = 7.5 Hz); HRMS (TOF-MS) *m/z* 544.1879 [M + H]⁺ (C₂₇H₃₁Cl₂N₅O₃ requires 544.1871).

(5R,6S)-5-(3-Chlorophenyl)-6-(4-chlorophenyl)-1-(2,4-dimethoxybenzyl)piperidin-2-one (44). To a suspension of NaH

(60% in mineral oil, 0.25 g, 6.25 mmol) in DMF (8.0 mL) was added (5*R*,6*S*)-**3** (1.00 g, 3.12 mmol) in DMF (2.0 mL) at 0 °C. The resulting reaction mixture was stirred at 0 °C for 45 min. Then freshly prepared 2,4-dimethoxybenzyl chloride[35] (1.34 g, 7.18 mmol) in DMF (3.0 mL) was added, and the resulting solution was slowly allowed to warm to 25 °C and stirred for 2.5 h. The reaction was quenched (ice-cold water) at 0 °C, extracted (2 × EtOAc), washed (3 × brine), and dried (MgSO$_4$). The combined organic layers were concentrated under reduced pressure. Flash column chromatography (SiO$_2$, 45% EtOAc/hexanes) gave **44** (1.25 g, 85% yield) as a white foam: ^{1}H NMR (400 MHz, CDCl$_3$) δ ppm 7.20 (2 H, d, *J* = 8.4 Hz), 7.03–7.09 (2 H, m), 6.96–7.02 (1 H, m), 6.86 (2 H, d, *J* = 8.4 Hz), 6.82–6.84 (1 H, m), 6.67 (1 H, d, *J* = 7.6 Hz), 6.30–6.39 (2 H, m), 5.20 (1 H, d, *J* = 14.5 Hz), 4.53 (1 H, d, *J* = 5.7 Hz), 3.72 (3 H, s), 3.59 (3 H, s), 3.53 (1 H, d, *J* = 14.3 Hz), 2.82–2.88 (1 H, m), 2.33–2.53 (2 H, m), 1.93–2.04 (1 H, m), 1.75–1.88 (1 H, m); MS (ESI) 470.2 [M + H]$^+$.

(5*R*,6*S*)-3-Allyl-5-(3-chlorophenyl)-6-(4-chlorophenyl)-1-(4-methoxybenzyl)-3-methylpiperidin-2-one (45). To a solution of **44** (525 mg, 1.12 mmol) and MeI (0.087 mL, 1.40 mmol) in THF (3.7 mL) was added LiHMDS (1 M in THF, 1.23 mL, 1.23 mmol) at −78 °C. After being stirred at −78 °C for 15 min, the mixture was allowed to warm to 25 °C and stirred overnight. The reaction was quenched (saturated aqueous NH$_4$Cl), extracted (2 × EtOAc), and washed (brine). The combined organic layers were dried (Na$_2$SO$_4$) and concentrated under reduced pressure. Flash column chromatography (SiO$_2$, 15–35% EtOAc/hexanes, gradient elution) provided (5*R*,6*S*)-5-(3-chlorophenyl)-6-(4-chlorophenyl)-1-(2,4-dimethoxybenzyl)-3-methylpiperidin-2-one (490 mg, 91% yield) as a colorless foam: MS (ESI) 484.2 [M + H]$^+$.

To a solution of the product above (474 mg, 0.979 mmol) and allyl bromide (745 μL, 8.81 mmol) in THF (4.8 mL) was added LiHMDS (1.0 M in THF, 7.83 mL, 7.83 mmol) at 25 °C. After being stirred for 5 min, the mixture was heated at 40 °C for 3 h. The reaction was quenched (saturated aqueous NH$_4$Cl), extracted (2 × EtOAc), and washed (brine). The combined organic layers were dried (Na$_2$SO$_4$) and concentrated under reduced pressure. Flash column chromatography (SiO$_2$, 10–30% EtOAc/hexanes, gradient elution) provided **45** (420 mg, 0.801 mmol, 82% yield, dr = 3.9:1 in favor of the desired isomer) as a colorless foam: MS (ESI) 524.2 [M + H]$^+$.

(3*S*,5*R*,6*S*)-3-Allyl-5-(3-chlorophenyl)-6-(4-chlorophenyl)-3-methylpiperidin-2-one (46). **45** (82 mg, 0.16 mmol) was dissolved in trifluoroacetic acid (1.2 mL, 16 mmol), and the resulting solution was stirred at 50 °C for 2 h. TFA was removed under reduced pressure, and the crude product was dissolved (10% MeOH/DCM), neutralized (saturated aqueous NaHCO$_3$), and filtered through Celite to remove insoluble material. Then the filtrate was extracted (2 × 10% MeOH/DCM) and washed (brine). The combined organic layers were dried (Na$_2$SO$_4$) and concentrated under reduced pressure. Flash column chromatography (SiO$_2$, 27–37% EtOAc/hexanes, gradient elution) provided the C3 epimer of **46** (13 mg, 22% yield) and **46** (41 mg, 70% yield) as white solids successively. C3 epimer of **46**: ^{1}H NMR (500 MHz, CDCl$_3$) δ ppm 7.19–7.23 (2 H, m), 7.16–7.18 (1 H, m), 7.10–7.14 (1 H, m), 7.00–7.03 (1 H, m), 6.93–6.97 (2 H, m), 6.76–6.80 (1 H, m), 5.78–5.86 (1 H, m), 5.69 (1 H, s, br), 5.15–5.22 (2 H, m), 4.45 (1 H, d, *J* = 10.8 Hz), 2.96–3.03 (1 H, m), 2.68–2.73 (1 H, m), 2.39 (1 H, t, *J* = 13.4 Hz), 2.23–2.29 (1 H, m), 1.71–1.75 (1 H, m), 1.45 (3 H, s); MS (ESI) 374.0 [M + H]$^+$. Compound **46**: ^{1}H NMR (500 MHz, CDCl$_3$) δ ppm 7.19–7.23 (2 H, m), 7.16–7.18 (1 H, m), 7.10–7.14 (1 H, m), 6.99–7.02 (1 H, m), 6.93–6.97 (2 H, m), 6.75–6.78 (1 H, m), 5.84–5.94 (1 H, m), 5.67 (1 H, s, br), 5.15–5.20 (2 H, m), 4.50 (1 H, d, *J* = 10.8 Hz), 3.03–3.10 (1 H, m), 2.59–2.65 (1 H, m), 2.52–2.56 (1 H, m), 2.02–2.12 (2 H, m), 1.31 (3 H, s); MS (ESI) 374.0 [M + H]$^+$.

(3*S*,5*R*,6*S*)-3-Allyl-5-(3-chlorophenyl)-6-(4-chlorophenyl)-3-methyl-1-(pentan-3-yl) piperidin-2-one (47). To a solution of **46** (100 mg, 0.267 mmol) in 3-bromopentane (1.0 mL, 8.0 mmol) was added sodium hydride (60% in mineral oil, 75 mg, 1.87 mmol) at 25 °C. After the mixture was heated at 120 °C for 2 days, the reaction was quenched (saturated aqueous NH$_4$Cl), extracted (2 × EtOAc), and washed (brine). The combined organic layers were dried (Na$_2$SO$_4$)

and concentrated under reduced pressure. Flash column chromatography (SiO$_2$, 10% EtOAc/hexanes) provided **47** (47 mg, 0.11 mmol, 40% yield) as a colorless foam: ^{1}H NMR (400 MHz, CDCl$_3$) δ ppm 7.22 (2 H, d, *J* = 8.2 Hz), 7.07–7.18 (2 H, m), 6.85–7.04 (3 H, m), 6.70 (1 H, d, *J* = 7.6 Hz), 5.80–5.93 (1 H, m), 5.12–5.21 (2 H, m), 4.30 (1 H, d, *J* = 10.6 Hz), 3.10–3.20 (1 H, m), 2.69–2.79 (1 H, m), 2.56–2.67 (2 H, m), 1.80–2.06 (4 H, m), 1.48–1.58 (1 H, m), 1.35–1.47 (1 H, m), 1.27 (3 H, s), 0.93 (3 H, t, *J* = 7.4 Hz), 0.54 (3 H, t, *J* = 7.5 Hz); MS (ESI) 444.1 [M + H]$^+$.

2-((3*R*,5*R*,6*S*)-5-(3-Chlorophenyl)-6-(4-chlorophenyl)-3-methyl-2-oxo-1-(pentan-3-yl)piperidin-3-yl)acetic Acid (27). **27** was prepared from **47** according to a similar procedure described for the synthesis of **3**: ^{1}H NMR (400 MHz, CDCl$_3$) δ ppm 7.24–7.27 (2 H, m), 7.07–7.19 (2 H, m), 6.85–7.05 (3 H, m), 6.68 (1 H, d, *J* = 7.6 Hz), 4.34 (1 H, d, *J* = 10.4 Hz), 3.01–3.13 (2 H, m), 2.67–2.78 (1 H, m), 2.16–2.27 (1 H, m), 1.98–2.04 (1 H, m), 1.85–1.97 (2 H, m), 1.51 (3 H, s), 1.38–1.49 (2 H, m), 0.95 (3 H, t, *J* = 7.3 Hz), 0.49 (3 H, t, *J* = 7.5 Hz); HRMS (ESI) *m/z* 462.1598 [M + H]$^+$ (C$_{25}$H$_{29}$Cl$_2$NO$_3$ requires 462.1604).

(*S*)-*tert*-Butyl 2-((3*S*,5*R*,6*S*)-3-Allyl-5-(3-chlorophenyl)-6-(4-chlorophenyl)-3-methyl-2-oxopiperidin-1-yl)butanoate (48). To a solution of **46** (310 mg, 0.828 mmol) in DMF (1.7 mL) was added NaH (60% in mineral oil, 133 mg, 3.31 mmol) at 0 °C. After the mixture was stirred at 0 °C for 20 min, *tert*-butyl 2-bromobutanoate (924 mg, 4.14 mmol) was added, and then the mixture was allowed to warm to 25 °C. After the mixture was stirred for 4 h, the reaction was quenched (saturated aqueous NH$_4$Cl), extracted (2 × EtOAc), and washed (3 × brine). The combined organic layers were dried (Na$_2$SO$_4$) and concentrated under reduced pressure. Flash column chromatography (SiO$_2$, 0–20% EtOAc/hexanes, gradient elution) provided **48** (257 mg, 60%) and Cα epimer of **48**, (*R*)-*tert*-butyl 2-((3*S*,5*R*,6*S*)-3-allyl-5-(3-chlorophenyl)-6-(4-chlorophenyl)-3-methyl-2-oxopiperidin-1-yl)butanoate (120 mg, 28%), as colorless foams successively. Compound **48**: ^{1}H NMR (400 MHz, CDCl$_3$) δ ppm 7.23 (2 H, d, *J* = 8.4 Hz), 7.07–7.17 (2 H, m), 6.97–7.05 (3 H, m), 6.74–6.77 (1 H, m), 5.81–5.92 (1 H, m), 5.15–5.22 (2 H, m), 4.57 (1 H, d, *J* = 10.8 Hz), 3.24–3.33 (1 H, m), 2.88–2.92 (1 H, m), 2.54–2.66 (2 H, m), 2.22–2.35 (1 H, m), 2.08–2.17 (1 H, m), 1.92–1.98 (1 H, m), 1.49–1.55 (1 H, m), 1.51 (9 H, s), 1.25 (3 H, s), 0.56 (3 H, t, *J* = 7.5 Hz); MS (ESI) 538.2 [M + Na]$^+$. Cα epimer of **48**: ^{1}H NMR (400 MHz, CDCl$_3$) δ ppm 7.20 (2 H, d, *J* = 8.2 Hz), 7.00–7.17 (4 H, m), 6.93–6.95 (1 H, m), 6.68–6.73 (1 H, m), 5.84–5.96 (1 H, m), 5.14–5.22 (2 H, m), 4.47 (1 H, d, *J* = 10.6 Hz), 3.18–3.26 (1 H, m), 3.06–3.12 (1 H, m), 2.53–2.68 (2 H, m), 1.88–2.13 (4 H, m), 1.46 (9 H, s), 1.28 (3 H, s), 0.98 (3 H, t, *J* = 7.6 Hz); MS (ESI) 538.2 [M + Na]$^+$.

2-((3*R*,5*R*,6*S*)-1-((*S*)-1-(*tert*-Butoxy)-1-oxo-butan-2-yl)-5-(3-chlorophenyl)-6-(4-chlorophenyl)-3-methyl-2-oxopiperidin-3-yl)acetic Acid (25). **25** was prepared from **48** according to a similar procedure described for the synthesis of **2**: ^{1}H NMR (400 MHz, CDCl$_3$) δ ppm 7.24–7.26 (2 H, m), 7.07–7.19 (2 H, m), 6.98–7.06 (3 H, m), 6.73–6.77 (1 H, m), 4.58 (1 H, d, *J* = 10.6 Hz), 3.20–3.28 (1 H, m), 2.92–3.02 (2 H, m), 2.76–2.82 (1 H, m), 2.22–2.36 (2 H, m), 2.08–2.15 (1 H, m), 1.47–1.52 (1 H, m), 1.50 (9 H, s), 1.46 (3 H, s), 0.54 (3 H, t, *J* = 7.5 Hz); HRMS (ESI) *m/z* 534.1808 [M + H]$^+$ (C$_{28}$H$_{33}$Cl$_2$NO$_5$ requires 534.1801).

(*S*)-*tert*-Butyl 2-((3*R*,5*R*,6*S*)-3-((1*H*-Tetrazol-5-yl)methyl)-5-(3-chlorophenyl)-6-(4-chlorophenyl)-3-methyl-2-oxopiperidin-1-yl)butanoate (26). **26** was prepared from **25** according to similar procedures described for the synthesis of **24**: ^{1}H NMR (400 MHz, CDCl$_3$) δ ppm 7.23–7.26 (2 H, m), 7.10–7.19 (2 H, m), 7.00–7.03 (1 H, m), 6.88–6.94 (2 H, m), 6.76–6.78 (1 H, m), 4.60 (1 H, d, *J* = 10.8 Hz), 3.43–3.60 (2 H, m), 3.22–3.31 (1 H, m), 3.13–3.17 (1 H, m), 2.29–2.42 (2 H, m), 2.18–2.25 (1 H, m), 1.49–1.52 (9 H, m), 1.34–1.40 (1 H, m), 1.32 (3 H, s), 0.55 (3 H, t, *J* = 7.4 Hz); HRMS (ESI) *m/z* 558.2031 [M + H]$^+$ (C$_{28}$H$_{33}$Cl$_2$N$_5$O$_3$ requires 558.2027).

(*S*)-Ethyl 2-((3*S*,5*R*,6*S*)-3-Allyl-5-(3-chlorophenyl)-6-(4-chlorophenyl)-3-methyl-2-oxopiperidin-1-yl)butanoate (49). **49** was prepared from **46** using ethyl 2-bromobutanoate according to a similar procedure described for the synthesis of **48**: ^{1}H NMR (400 MHz,

CDCl$_3$) δ ppm 7.23 (2 H, d, J = 8.2 Hz), 7.07–7.17 (2 H, m), 6.92–7.05 (3 H, m), 6.74–6.77 (1 H, m), 5.80–5.92 (1 H, m), 5.14–5.23 (2 H, m), 4.57 (1 H, d, J = 10.8 Hz), 4.10–4.25 (2 H, m), 3.26–3.33 (1 H, m), 3.07–3.12 (1 H, m), 2.60 (2 H, d, J = 7.4 Hz), 2.22–2.33 (1 H, m), 2.03–2.18 (1 H, m), 1.94–1.99 (1 H, m), 1.58–1.68 (1 H, m), 1.30 (3 H, t, J = 7.1 Hz), 1.24 (3 H, s), 0.60 (3 H, t, J = 7.5 Hz); MS (ESI) 488.2 [M + H]$^+$.

(3S,5R,6S)-3-Allyl-5-(3-chlorophenyl)-6-(4-chlorophenyl)-1-((S)-1-hydroxybutan-2-yl)-3-methylpiperidin-2-one (50). To a solution of **49** (3.35 g, 6.86 mmol) in Et$_2$O (55 mL) was added LiBH$_4$ (299 mg, 13.7 mmol) at 0 °C. After the mixture was stirred at 0 °C for 30 min, the reaction was quenched (saturated aqueous NH$_4$Cl), extracted (2 × EtOAc), and washed (brine). The combined organic layers were dried (MgSO$_4$) and concentrated under reduced pressure. Flash column chromatography (SiO$_2$, 40–60% EtOAc/hexanes, gradient elution) provided **50** (2.10 g, 69% yield) as a colorless foam: ^{1}H NMR (400 MHz, CDCl$_3$) δ ppm 7.24 (2 H, d, J = 8.4 Hz), 7.07–7.19 (2 H, m), 6.95–7.04 (3 H, m), 6.68–6.74 (1 H, m), 5.80–5.92 (1 H, m), 5.13–5.22 (2 H, m), 4.46 (1 H, d, J = 10.2 Hz), 3.58–3.66 (2 H, m), 3.12–3.24 (2 H, m), 2.61 (2 H, d, J = 7.4 Hz), 1.91–2.07 (3 H, m), 1.39–1.51 (1 H, m), 1.27 (3 H, s), 0.68 (3 H, t, J = 7.5 Hz); MS (ESI) 446.1 [M + H]$^+$.

2-((3R,5R,6S)-5-(3-Chlorophenyl)-6-(4-chlorophenyl)-1-((S)-1-hydroxybutan-2-yl)-3-methyl-2-oxopiperidin-3-yl)acetic Acid (28). To a solution of **50** (630 mg, 1.41 mmol) and imidazole (240 mg, 3.52 mmol) in DMF (9 mL) was added *tert*-butyl diphenylchlorosilane (485 μL, 1.85 mmol) slowly at 25 °C. After the mixture was stirred for 16 h, the reaction was quenched (water), extracted (2 × EtOAc), and washed (3 × brine). The combined organic layers were dried (MgSO$_4$) and concentrated under reduced pressure. Flash column chromatography (SiO$_2$, 0–10% EtOAc/hexanes, gradient elution) provided (3S,5R,6S)-3-allyl-5-(3-chlorophenyl)-6-(4-chlorophenyl)-1-((S)-1-(2,2-dimethyl-1,1-diphenylpropoxy)butan-2-yl)-3-methylpiperidin-2-one (850 mg, 90% yield) as a colorless foam: MS (ESI) 684.2 [M + H]$^+$.

To a rapidly stirring solution of the TBDPS protected alcohol above (388 mg, 2.90 mmol) and RuCl$_3$ hydrate (19 mg, 0.085 mmol) in H$_2$O/CCl$_4$/AcCN (1.5:1:1, 7 mL) was added NaIO$_4$ (606 mg, 2.83 mmol) in four portions over 20 min while maintaining the temperature below 25 °C. After being stirred vigorously for 4 h, the mixture was filtered through Celite and the filter cake was washed (EtOAc). The filtrate was extracted (2 × EtOAc) and washed (2 × 10% aqueous NaHSO$_3$ and 1 × brine). The combined organic layers were dried (Na$_2$SO$_4$) and concentrated under reduced pressure. Purification by flash column chromatography (SiO$_2$, 0–20% MeOH/DCM, gradient elution) provided 2-((3R,5R,6S)-5-(3-chlorophenyl)-6-(4-chlorophenyl)-1-((S)-1-(2,2-dimethyl-1,1-diphenylpropoxy)-butan-2-yl)-3-methyl-2-oxopiperidin-3-yl)acetic acid (317 mg, 80% yield) as a pale brown foam: MS (ESI) 702.2 [M + H]$^+$.

To a solution of the product above (317 mg, 0.451 mmol) in THF (13 mL) was added tetrabutylammonium fluoride (1.0 M in THF, 2.2 mL, 2.2 mmol) slowly at 0 °C. After the mixture was stirred at 25 °C for 16 h, the reaction was quenched (1 N aqueous HCl) and extracted (2 × EtOAc). The combined organic layers were dried (Na$_2$SO$_4$) and concentrated under reduced pressure, and purification by RP-HPLC (10–90% A/B, gradient elution) provided **28** (1.03 g, 78% yield) as a white solid: ^{1}H NMR (500 MHz, CDCl$_3$) δ ppm 7.24–7.26 (2 H, m), 7.15–7.19 (1 H, m), 7.08–7.13 (1 H, m), 6.94–7.08 (3 H, m), 6.72–6.77 (1 H, m), 4.56 (1 H, d, J = 9.8 Hz), 3.72–3.81 (1 H, m), 3.60–3.65 (1 H, m), 3.19–3.27 (1 H, m), 3.08–3.15 (1 H, m), 2.97–3.04 (1 H, m), 2.73–2.78 (1 H, m), 2.16–2.26 (1 H, m), 2.04–2.11 (1 H, m), 1.88–1.99 (1 H, m), 1.43–1.50 (1 H, m), 1.47 (3 H, s), 0.63 (3 H, t, J = 7.2 Hz); HRMS (ESI) m/z 464.1386 [M + H]$^+$ (C$_{24}$H$_{27}$Cl$_2$NO$_4$ requires 464.1397).

(3S,5R,6S)-3-Allyl-5-(3-chlorophenyl)-6-(4-chlorophenyl)-1-((3S)-2-hydroxypentan-3-yl)-3-methylpiperidin-2-one (51). To a solution of **50** (5.87 g, 13.2 mmol) and water (360 μL, 19.7 mmol) in DCM (167 mL) was added Dess–Martin periodinane (8.37 g, 19.7 mmol) at 25 °C. After the mixture was stirred for 1.5 h, the reaction was quenched (aqueous 1 M Na$_2$S$_2$O$_3$), extracted (2 × DCM), and

washed (2 × saturated aqueous NaHCO$_3$ and 2 × brine). The combined organic layers were dried (Na$_2$SO$_4$) and concentrated under reduced pressure. Flash column chromatography (SiO$_2$, 20%, 25%, and 30% EtOAc/hexanes) provided (S)-2-((3S,5R,6S)-3-allyl-5-(3-chlorophenyl)-6-(4-chlorophenyl)-3-methyl-2-oxopiperidin-1-yl)butanal (4.61 g, 79% yield) as a colorless film: ^{1}H NMR (400 MHz, CDCl$_3$) δ ppm 9.50 (1 H, s), 7.24 (2 H, d, J = 8.2 Hz), 7.06–7.17 (2 H, m), 6.93–7.06 (3 H, m), 6.77 (1 H, d, J = 7.4 Hz), 5.80–5.95 (1 H, m), 5.17–5.25 (2 H, m), 4.54 (1 H, d, J = 10.8 Hz), 3.26–3.35 (1 H, m), 3.14–3.19 (1 H, m), 2.62 (2 H, d, J = 7.4 Hz), 2.10–2.28 (2 H, m), 1.96–2.04 (1 H, m), 1.46–1.58 (1 H, m), 1.26 (3 H, s), 0.69 (3 H, t, J = 7.6 Hz); MS (ESI) 444.1 [M + H]$^+$.

To a solution of the aldehyde above (5.20 g, 11.7 mmol) in THF (117 mL) was added MeMgBr (1.4 M in toluene/THF (75:25), 25 mL, 35 mmol) at 0 °C. The mixture was allowed to warm to 25 °C and stirred for 1 h. The reaction was quenched (aqueous saturated NH$_4$Cl), extracted (2 × EtOAc), and washed (2 × brine). The combined organic layers were dried (Na$_2$SO$_4$) and concentrated under reduced pressure. Flash column chromatography (SiO$_2$, 30% and 50% EtOAc/hexanes) provided **51** (4.70 g, 87% yield) as a pale yellow foam (dr = 4:6 in favor of the *R*-isomer): MS (ESI) 460.2 [M + H]$^+$.

2-((3R,5R,6S)-5-(3-Chlorophenyl)-6-(4-chlorophenyl)-3-methyl-2-oxo-1-((S)-2-oxopentan-3-yl)-piperidin-3-yl)acetic Acid (52). To a rapidly stirring solution of **51** (3.14 g, 6.82 mmol) and RuCl$_3$·hydrate (31 mg, 0.14 mmol) in water/AcCN/CCl$_4$ (1.5:1:1, 98 mL) was added NaIO$_4$ (8.75 g, 40.9 mmol) in six portions over 1 h while maintaining the temperature below 25 °C. The mixture was stirred for an additional 1 h after the final addition of NaIO$_4$. The mixture was filtered through Celite, and the filter cake was washed (EtOAc). The filtrate was extracted (2 × EtOAc) and washed (2 × 10% aqueous NaHSO$_3$ and 1 × brine). The combined organic layers were dried (Na$_2$SO$_4$) and concentrated under reduced pressure. Flash column chromatography [SiO$_2$, 10–50% (15% MeOH/acetone)/hexanes] provided **52** (2.59 g, 80% yield) as a light pink foam: ^{1}H NMR (400 MHz, CDCl$_3$) δ ppm 7.24 (2 H, d, J = 8.2 Hz), 7.06–7.16 (2 H, m), 6.95–7.04 (3 H, m), 6.74–6.76 (1 H, m), 4.47 (1 H, d, J = 10.8 Hz), 3.25–3.33 (1 H, m), 3.12–3.17 (1 H, m), 2.82–2.93 (2 H, m), 2.28–2.35 (1 H, m), 2.12–2.22 (2 H, m), 2.16 (3 H, s), 1.78–1.86 (1 H, m), 1.47 (3 H, s), 0.64 (3 H, t, J = 7.5 Hz); HRMS (ESI) m/z 476.1407 [M + H]$^+$ (C$_{25}$H$_{27}$Cl$_2$NO$_4$ requires 476.1397).

2-((3R,5R,6S)-5-(3-Chlorophenyl)-6-(4-chlorophenyl)-1-((2S,3S)-2-hydroxypentan-3-yl)-3-methyl-2-oxopiperidin-3-yl)-acetic Acid (29). To a solution of **52** (3.86 g, 8.13 mmol) in THF (102 mL) was added L-Selectride (1 M in THF, 16.3 mL, 16.3 mmol) dropwise over 5 min at −78 °C. After being stirred at −78 °C for 30 min, the mixture was allowed to warm to 25 °C and stirred for 2 h. The reaction was quenched (saturated aqueous NH$_4$Cl), extracted (3 × EtOAc), and washed (3 × ice-cold 1 N aqueous HCl and 3 × brine). The combined organic layers were dried (Na$_2$SO$_4$) and concentrated under reduced pressure. Flash column chromatography [SiO$_2$, 10–30% (15% MeOH/acetone) in hexanes, a gradient elution] and recrystallization (hexanes/acetone = 3:1) provided **29** (2.90 g, 75% yield) as a white solid: ^{1}H NMR (500 MHz, DMSO-d$_6$) δ ppm 12.42 (1 H, br s), 7.33 (2 H, d, J = 8.4 Hz), 7.17–7.27 (4 H, m), 7.08–7.10 (1 H, m), 6.93–6.95 (1 H, m), 4.80 (1 H, br s), 4.77 (1 H, d, J = 10.9 Hz), 4.01–4.06 (1 H, m), 3.35–3.40 (1 H, m), 2.87 (1 H, d, J = 13.7 Hz), 2.48 (1 H, d, J = 13.7 Hz), 2.29–2.33 (1 H, m), 2.04–2.15 (2 H, m), 1.55–1.64 (1 H, m), 1.41–1.49 (1 H, m), 1.26 (3 H, s), 1.00 (3 H, d, J = 6.3 Hz), 0.30 (3 H, t, J = 7.6 Hz); HRMS (ESI) m/z 478.1560 [M + H]$^+$ (C$_{25}$H$_{29}$Cl$_2$NO$_4$ requires 478.1553); [α]$^{23}_D$ +110° (c 0.51, MeOH).

■ ASSOCIATED CONTENT

Ⓢ Supporting Information

(i) ^{1}H NMR spectra of **23** and **25** at 298 and 203 K, (ii) in vitro biological assays, (iii) in vivo study protocols, (iv) determination of cocrystal structures of **23** and **29** with MDM2, and (v) structures and energies of the gauche and anti conformers

in Figure 7. This material is available free of charge via the Internet at http://pubs.acs.org.

■ AUTHOR INFORMATION

Corresponding Author

*Telephone: 650-244-2195. Fax: 650-837-9369. E-mail: daqings@amgen.com.

Notes

The authors declare no competing financial interest.

■ ABBREVIATIONS USED

AcCN, acetonitrile; b.i.d., twice a day dosing; Boc, tert-butoxycarbonyl; BrdU, 5-bromo-2-deoxyuridine; CL, clearance; CYP3A4, cytochrome P450 3A4; DCM, dichloromethane; DMBCl, 2,4-dimethoxybenzyl chloride; DMF, N,N-diemethyl-formamide; DMSO, dimethylsulfoxide; dr, diastereoselectivity ratio; EdU, 5-ethynyl-2'-deoxyuridine; EtOAc, ethyl acetate; FACS, fluorescence-activated cell sorting; hPXR, human pregnane X receptor; HTRF, homogeneous time-resolved fluorescence; LiHMDS, lithium bis(trimethylsilyl)amide; MDM2, murine double minute 2; MsCl, methanesulfonyl chloride; NaHMDS, sodium bis(trimethylsilyl)amide; NMO, N-methylmorpholinine N-oxide; q.d., once a day dosing; qRT-PCR, quantitative reverse transcription polymerase chain reaction; SEM, standard error of the mean; SPR, surface plasmon resonance; TBAF, tetrabutylammonium fluoride; TDI, time dependent inhibition; TEA, triethylamine; TFA, trifluoro-acetic acid; THF, tetrahydrofuran

■ REFERENCES

(1) Vazquez, A.; Bond, E. E.; Levine, A. J.; Bond, G. L. The genetics of the p53 pathway, apoptosis and cancer therapy. Nat. Rev. Drug Discovery 2008, 7, 979–987.

(2) Chene, P. Inhibiting the p53-MDM2 interaction: an important target for cancer therapy. Nat. Rev. Cancer 2003, 3, 102–109.

(3) Vogelstein, B.; Lane, D.; Levine, A. J. Surfing the p53 network. Nature (London) 2000, 408, 307–310.

(4) Kastan, M. B. Wild-type p53: tumors can't stand it. Cell 2007, 128, 837–840.

(5) Ventura, A.; Kirsch, D. G.; McLaughlin, M. E.; Tuveson, D. A.; Grimm, J.; Lintault, L.; Newman, J.; Reczek, E. E.; Weissleder, R.; Jacks, T. Restoration of p53 function leads to tumor regression in vivo. Nature (London) 2007, 445, 661–665.

(6) Xue, W.; Zender, L.; Miething, C.; Dickins, R. A.; Hernando, E.; Krizhanovsky, V.; Cordon-Cardo, C.; Lowe, S. W. Senescence and tumour clearance is triggered by p53 restoration in murine liver carcinomas. Nature (London) 2007, 445, 656–660.

(7) Martins, C. P.; Brown-Swigart, L.; Evan, G. I. Modeling the therapeutic efficacy of p53 restoration in tumors. Cell 2006, 127, 1323–1334.

(8) Hollstein, M.; Sidransky, D.; Vogelstein, B.; Harris, C. C. p53 Mutations in human cancers. Science (Washington, D.C.) 1991, 253, 49–53.

(9) Vassilev, L. T. p53 Activation by small molecules: application in oncology. J. Med. Chem. 2005, 48, 4491–4499.

(10) Arkin, M. R.; Wells, J. A. Small-molecule inhibitors of protein-protein interactions: progressing towards the dream. Nat. Rev. Drug Discovery 2004, 3, 301–317.

(11) Information from www.clinicaltrials.gov. (a) RG7112 (Hoffmann-La Roche). (b) RO5503781 (Hoffmann-La Roche). (c) MK-8242 (Merck).

(12) Allen, J. G.; Bourbeau, M. P.; Wohlhieter, G. E.; Bartberger, M. D.; Michelsen, K.; Hungate, R.; Gadwood, R. C.; Gaston, R. D.; Evans, B.; Mann, L. W.; Matison, M. E.; Schneider, S.; Huang, X.; Yu, D.; Andrews, P. S.; Reichelt, A.; Long, A. M.; Yakowec, P.; Yang, E. Y.; Lee, T. A.; Oliner, J. D. Discovery and optimization of chromeno-triazolopyrimidines as potent inhibitors of the mouse double minute 2-tumor protein 53 protein−protein interaction. J. Med. Chem. 2009, 52, 7044−7053.

(13) Beck, H. P.; DeGraffenreid, M.; Fox, B.; Allen, J. G.; Rew, Y.; Schneider, S.; Saiki, A. Y.; Yu, D.; Oliner, J. D.; Salyers, K.; Ye, Q.; Olson, S. Improvement of the synthesis and pharmacokinetic properties of chromenotriazolopyrimidine MDM2-p53 protein−protein inhibitors. Bioorg. Med. Chem. Lett. 2011, 21, 2752−2755.

(14) Vassilev, L. T.; Vu, B. T.; Graves, B.; Carvajal, D.; Podlaski, F.; Filipovic, Z.; Kong, N.; Kammlott, U.; Lukacs, C.; Klein, C.; Fotouhi, N.; Liu, E. A. In vivo activation of the p53 pathway by small-molecule antagonists of MDM2. Science (Washington, D.C.) 2004, 303, 844−848.

(15) Shangary, S; Qin, D.; McEachern, D.; Liu, M.; Miller, R. S.; Qiu, S.; Nikolovska-Coleska, Z.; Ding, K.; Wang, G.; Chen, J.; Bernard, D.; Zhang, J.; Lu, Y.; Gu, Q.; Shah, R. B.; Pienta, K. J.; Ling, X.; Kang, S.; Guo, M.; Sun, Y.; Yang, D.; Wang, S. Temporal activation of p53 by a specific MDM2 inhibitor is selectively toxic to tumors and leads to complete tumor growth inhibition. Proc. Natl. Acad. Sci. U.S.A. 2008, 105, 3933−3938.

(16) Experimental details of the in vitro biological assays can be found in the Supporting Information.

(17) Kussie, P. H.; Gorina, S; Marechal, V; Elenbaas, B; Moreau, J.; Levine, A. J.; Pavletich, N. P. Structure of the MDM2 oncoprotein bound to the p53 tumor suppressor transactivation domain. Science (Washington, D.C.) 1996, 274, 948−953.

(18) Popowicz, G. M.; Dömling, A.; Holak, T. A. The structure-based design of Mdm2/Mdmx−p53 inhibitors gets serious. Angew. Chem., Int. Ed. 2011, 50, 2680−2688.

(19) When the TFA salt of MI-63 was in organic solvents (MeOH and DMSO), the quaternary carbon center of the spirolactam system and the tert-butyl group were slowly isomerized (in-house result).

(20) Detailed analysis of these scaffolds and SAR studies leading to both 1 and 2 will be reported in a separate communication.

(21) The absolute stereochemistry of compound 2 was assigned via comparison of theoretical and experimental VCD and optical rotations of the C3-allyl precursors of both compound 2 and its enantiomer. Detailed studies will be reported in a separate communication.

(22) Docking was performed via alignment of 2 to various MDM2 cocrystallized ligands with the in-house flexible alignment tool FLAME.[37] The resultant structures were subject to minimization in the MDM2 protein using AMBER, version 9.0.[38] Top-scoring poses gave rise to the model depicted in Figure 3.

(23) El-Deiry, W. S.; Tokino, T.; Velculescu, V. E.; Levy, D. B.; Parsons, R; Trent, J. M.; Lin, D.; Mercer, W. E.; Kinzler, K. W.; Vogelstein, B. WAF1, a potential mediator of p53 tumor suppression. Cell 1993, 75, 817−825.

(24) Bunz, F.; Dutriaux, A.; Lengauer, C.; Waldman, T.; Zhou, S.; Brown, J. P.; Sedivy, J. M.; Kinzler, K. W.; Vogelstein, B. Requirement for p53 and p21 to sustain G2 arrest after DNA damage. Science (Washington, D.C.) 1998, 282, 1497−1501.

(25) Hastak, K.; Agarwal, M. K.; Mukhtar, H.; Agarwal, M. L. Ablation of either p21 or Bax prevents p53-dependent apoptosis induced by green tea polyphenol epigallocatechin-3-gallate. FASEB J. 2005, 19, 789−791.

(26) Fujiwara, K.; Daido, S.; Yamamoto, A.; Kobayashi, R.; Yokoyama, T.; Aoki, H.; Iwado, E.; Shinojima, N.; Kondo, Y.; Kondo, S. Pivotal role of the cyclin-dependent kinase inhibitor

p21WAF1/CIP1 in apoptosis and autophagy. *J. Biol. Chem.* **2008**, *283*, 388−397.

(27) The atomic coordinates have been deposited in the Protein Data Bank under an accession code 4ERE.

(28) MP2 and M06-2X single-point energy calculations utilizing the 6-31G* and cc-PVDZ basis sets support the B3LYP/6-31G* predictions. All quantum mechanical calculations were performed using the Gaussian 03 and Gaussian 09 program systems. See Supporting Information.

(29) ^{1}H NMR spectra can be found in the Supporting Information.

(30) Experimental details of in vivo studies can be found in the Supporting Information.

(31) Detailed SAR studies will be reported in separate communications.

(32) The atomic coordinates have been deposited in the Protein Data Bank under an accession code 4ERF.

(33) All of the stereochemistry were assigned based on the cocrystal structure of the fully functionalized **22** (unpublished result), **23**, or **29** with human MDM2 protein.

(34) Relative stereochemistry of the C3 carbon of the piperidinone core in both allyl and homoallyl derivatives was determined by NOE experiments between two protons at the C3 and C5 positions.

(35) Elliott, J. D.; Gleason, J. G.; Hill, D. T. Patent US 5817653 A1, 1998; SmithKline Beecham Corporation.

(36) The stereochemistry of the methyl carbinol was confirmed by additional synthetic studies of **29**, which will be discussed in a separate communication.

(37) Cho, S. J.; Sun, Y. FLAME, a program to flexibly align molecules. *J. Chem. Inf. Model.* **2006**, *46*, 298−306.

(38) Case, D. A.; Darden, T. A.; Cheatham, T. E., III; Simmerling, C. L.; Wang, J.; Duke, R. E.; Luo, R.; Merz, K. M.; Pearlman, D. A.; Crowley, M.; Walker, R. C.; Zhang, W.; Wang, B.; Hayik, S.; Roitberg, A.; Seabra, G.; Wong, K. F.; Paesani, F.; Wu, X.; Brozell, S.; Tsui, V.; Gohlke, H.; Yang, L.; Tan, C.; Mongan, J.; Hornak, V.; Cui, G.; Beroza, P.; Mathews, D. H.; Schafmeister, C.; Ross, W. S.; Kollman, P. A. *AMBER*, version 9; University of California—San Francisco, CA, 2006.